A mouse model of Bardet-Biedl Syndrome has impaired fear memory, which is rescued by lithium treatment

Thomas K. Pak*[1,2,3,16], Calvin S. Carter*[3], Qihong Zhang[3], Sunny C. Huang[1,3], Charles Searby[3], Ying Hsu[3], Rebecca Taugher[4,5], Tim Vogel[3], Christopher C. Cychosz[6], Rachel Genova[1], Nina Moreira[8], Hanna Stevens[2,4], John Wemmie[2,4,5,7], Andrew A. Pieper[9-14], Kai Wang[15], Val C. Sheffield[2,3]

1 Medical Scientist Training Program, Roy J. and Lucille A. Carver College of Medicine, University of Iowa, Iowa City, IA, USA

2 Neuroscience Program, Roy J. and Lucille A. Carver College of Medicine, University of Iowa, Iowa City, IA, USA

3 Department of Pediatrics, Roy J. and Lucille A. Carver College of Medicine, University of Iowa, Iowa City, IA, USA

4 Department of Psychiatry, Roy J. and Lucille A. Carver College of Medicine, University of Iowa, Iowa City, IA, USA

5 Department of Veterans Affairs Medical Center, Iowa City, IA, USA

6 Department of Orthopedics, Roy J. and Lucille A. Carver College of Medicine, University of Iowa, Iowa City, IA, USA

7 Department of Molecular Physiology and Biophysics, Roy J. and Lucille A. Carver College of Medicine, University of Iowa, Iowa City, IA, USA

8 Department of Obstetrics and Gynecology, Roy J. and Lucille A. Carver College of Medicine, University of Iowa, Iowa City, IA, USA

9 Harrington Discovery Institute, University Hospitals Cleveland Medical Center, Cleveland, OH, USA

10 Department of Psychiatry, Case Western Reserve University, Cleveland, OH, USA

11 Geriatric Psychiatry, GRECC, Louis Stokes Cleveland VA Medical Center; Cleveland, OH, USA

12 Institute for Transformative Molecular Medicine, School of Medicine, Case Western Reserve University, Cleveland, OH, USA

13 Weill Cornell Autism Research Program, Weill Cornell Medicine of Cornell University, NY, USA

14 Department of Neuroscience, Case Western Reserve University, School of Medicine, Cleveland, OH, USA

15 Department of Biostatistics, College of Public Health, University of Iowa, Iowa City, IA, USA

16 Corresponding author, Thomas-pak@uiowa.edu

*These authors contributed equally to this work

Data Availability: All relevant data are within the paper and its Supporting Information files. Additional data that support the findings of this study are available from the corresponding author upon reasonable request.

Competing interests: The authors have declared that no competing interests exist.

Funding: This work was supported by NIH grants RO1 EY011298 and R01 EY017168 (to V.C.S.), and the Roy J. Carver Charitable Trust (V.C.S.). The work was also supported and greatly facilitated by the core facilities funded by NIH grant P30 EY025580 (PI: V.C.S.). AAP was supported by the Brockman Foundation, the Elizabeth Ring Mather & William Gwinn Mather Fund, S. Livingston Samuel Mather Trust, G.R. Lincoln Family Foundation, Wick Foundation, the Leonard Krieger Fund of the Cleveland Foundation, Gordon & Evie Safran, the Louis Stokes VA Medical Center resources and facilities, project 19PABH134580006-AHA/Allen Initiative in Brain Health and Cognitive Impairment, NIH-NIA RO1AG066707 and the Translational Therapeutics Core of the Cleveland Alzheimer's Disease Research Center (NIH/NIA: 1 P30 AGO62428-01).

Abstract

Primary cilia are microtubule-based organelles present on most cells that regulate many physiological processes, ranging from maintaining energy homeostasis to renal function. However, the role of these structures in the regulation of behavior remains unknown. To study the role of cilia in behavior, we employ mouse models of the human ciliopathy, Bardet-Biedl Syndrome (BBS). Here, we demonstrate that BBS mice have significant impairments in context fear conditioning, a form of associative learning. Moreover, we show that postnatal deletion of BBS gene function, as well as congenital deletion, specifically in the forebrain, impairs context fear conditioning. Analyses indicated that these behavioral impairments are not the result of impaired hippocampal long-term potentiation. However, our results indicate that these behavioral impairments are linked to impaired hippocampal neurogenesis. Two-week treatment with lithium chloride partially restores the proliferation of hippocampal neurons which leads to a rescue of context fear conditioning. Overall, our results identify a novel role of cilia genes in hippocampal neurogenesis and long-term context fear conditioning.

Author summary

The primary cilium is a microtubule-based membranous projection on the cell that is involved in multiple physiological functions. Patients who have cilia dysfunction commonly have intellectual disability. However, it is not known how cilia affect learning and memory. Studying mouse models of a cilia-based intellectual disability can provide insight into learning and memory. One such cilia-based intellectual disability is Bardet-Biedl Syndrome (BBS), which is caused by homozygous and compound heterozygous mutations of BBS genes. We found that a mouse model of BBS (*Bbs1*$^{M390R/M390R}$ mice) has learning and memory defects. In addition, we found that other mouse models of BBS have similar learning and memory defects. These BBS mouse models have difficulty associating an environment with an aversive

78 stimulus, a task designed to test context fear memory. This type of memory involves the hippocampus.
79 We found that *Bbs1*$^{M390R/M390R}$ mice have decreased cell production in the hippocampus. Treating
80 *Bbs1*$^{M390R/M390R}$ mice with a compound (lithium) that increases cell production in the hippocampus
81 improved the learning and memory deficits. Our results demonstrate a potential role for cilia in learning
82 and memory, and indicate that lithium is a potential treatment, requiring further study, for the intellectual
83 disability phenotype of BBS.
84

Introduction

Intellectual disability (ID) is one of the most common neurodevelopmental disorders, affecting 1% of the global population [1, 2]. Clinically, ID is characterized by a deficit in intellectual functioning and adaptive functioning [3]. There are limited pharmacological interventions for ID, partially due to the heterogeneous nature of ID, and a poor understanding of ID which can be attributed to a lack of animal models of ID [4, 5]. There is an urgent need to develop animal models to improve our understanding of the pathophysiological mechanisms underlying this pervasive condition.

Patients with abnormal cilia, i.e. ciliopathies, frequently present with ID, suggesting that cilia play an important role in learning and memory, yet the mechanisms underlying the phenotype remain unknown [6]. Primary cilia are microtubule-based structures that extend from the surface of nearly all cells in the body, including neurons. Cilia play a role in maintaining energy homeostasis and facilitating physiological responses to sensory stimuli [7]. There are robust mouse models of ciliopathies that recapitulate the primary features of the human ciliopathies, which allow us to study the role of cilia in learning and memory. To this end, we employed mouse models of the human ciliopathy, Bardet-Biedl Syndrome (BBS), which presents clinically with intellectual disability [8] in order to investigate the role of cilia in learning and memory.

BBS is a genetically heterogenous autosomal recessive ciliopathy with 22 known causative genes [9]. Clinical features of BBS include rod-cone dystrophy progressing to blindness, postaxial polydactyly, obesity, renal anomalies, and intellectual disability [10]. BBS proteins are involved in ciliary function. Eight BBS genes, specifically *BBS1*, *BBS2*, *BBS4*, *BBS5*, *BBS7*, *BBS8*, *BBS9*, and *BBS18* (*BBIP1*), encode the components of the BBSome [11, 12], an octameric protein complex. The BBSome regulates ciliary trafficking of G-Protein Coupled Receptors (GPCR) including SMO[13], NPY2R [14], MCHR1 and SSTR3[15], and D1R [16]), as well as non-GPCRs (TRKB[17]). Three non-BBSome BBS proteins

(BBS6, BBS10, and BBS12) form a complex that mediates the assembly of the BBSome [18]. BBS3 is a GTPase that is also involved in ciliary receptor trafficking[19].

We have developed multiple mouse models of BBS [20]. Unlike some other ciliopathy mouse models, BBS models are viable and clinically relevant because they use mutations found in human patients [21-24]. We focused on the use of *Bbs1*$^{M390R/M390R}$ mice, harboring the most common human BBS mutation, as it recapitulates many of BBS phenotypes present in patients, including obesity, retinopathy, and decreased hippocampal volume[24, 25]. Despite the phenotypic association between decreased hippocampal volume in patients and the known role of the hippocampus in learning and memory, the role of BBS in learning and memory is not well studied. Here, we investigate the role of these cilia genes in learning and memory using a fear conditioning paradigm.

Fear conditioning evaluates associative learning and involves pairing a neutral stimulus [conditioned stimulus (CS)], to an aversive stimulus [unconditioned stimulus (US)]. Fear conditioning is commonly used to understand the neurobiological mechanisms of ID as well as fear learning and memory in mice due to several advantages [26-29] . First, fear conditioning paradigms provide distinct insights into the neural correlates of learning and memory, for example, context or cue-dependent conditioning, which require contributions from different brain regions [30]. Second, the pairing of CS to US consistently elicits a measurable set of physiological and behavioral responses [31]. Third, fear conditioning allows for the delineation between short-term and long-term memory performance, depending on the time duration from training to testing. To assess short-term context fear conditioning, a one-hour interval between training and testing is utilized. To evaluate long-term context fear conditioning, an interval $\geq$ 24 hours is utilized [32-34]. Finally, fear conditioning is a form of passive learning, making it an accessible behavioral test for mice with motor deficits [35].

Here, we report that *Bbs1*$^{M390R/M390R}$ mice have impaired long-term context fear conditioning, but normal short-term context memory. In addition, we show that multiple BBS mouse models have impaired long-term context fear conditioning, including a mouse model with preferential deletion of *Bbs1* in the forebrain. We also show a novel role for BBS genes in neural proliferation and neurogenesis in the hippocampus. In addition, we show that two-week treatment with lithium chloride rescues long-term context fear conditioning and partially rescues hippocampal neurogenesis in *Bbs1*$^{M390R/M390R}$ mice. Overall, this study shows a molecular connection between primary cilia and learning and memory using mouse models of BBS. Our study also identifies lithium as a potential therapeutic agent for treating the intellectual disability aspect of BBS.

Results

1. *Bbs1*$^{M390R/M390R}$ mice have impaired long-term fear conditioning.

To study role of BBS in learning and memory, we employed a mouse model of the most common human BBS mutation, *Bbs1*$^{M390R/M390R}$. Learning was evaluated using a three-day delay fear conditioning paradigm, which tests for long term association memory (Fig 1A). Controls were littermate heterozygote or wild-type mice as there is no difference in fear conditioning between these animals (S1 Fig). On day 1, both *Bbs1*$^{M390R/M390R}$ mice and their littermate controls showed increased freezing behavior following a shock stimulus, indicating that BBS mice exhibit a normal physiological response to an aversive stimulus (Fig 1B). On day 2 (post 24 hours from training), mice were introduced into a novel environment to test cue (sound) dependent fear conditioning. We found no significant differences between *Bbs1*$^{M390R/M390R}$ and control mice, indicating that BBS mice have intact cue dependent learning (Fig 1C). On day 3 (post 48 hours from training), mice were re-introduced back into the training environment to test context (environment) dependent learning. Remarkably, *Bbs1*$^{M390R/M390R}$ mice showed a 28% reduction in freeze behavior in this environment relative to littermate controls (Fig 1C). A sex difference was not observed in control mice or *Bbs1*$^{M390R/M390R}$ mice for acquisition (immediate fear conditioning), cue fear conditioning (24 hours after acquisition), and context fear conditioning (48 hours after acquisition) (S2 Fig). These findings revealed that BBS mice have context specific fear conditioning impairments.

Due to the pleiotropic nature of BBS, we tested for confounding factors that may underlie the striking impairments in fear conditioning observed in *Bbs1*$^{M390R/M390R}$ mice. No hearing differences were observed between *Bbs1*$^{M390R/M390R}$ mice and control mice based on Auditory Brainstem Response and hearing behavior (S3A and S3B Fig). No differences were observed in shock reactivity between *Bbs1*$^{M390R/M390R}$ mice and control mice indicating a normal tactile response (S3C Fig). Moreover, we did not observe a

difference in activity levels or sleep behavior between *Bbs1*$^{M390R/M390R}$ mice and control mice (S3D and S3E Fig). These findings revealed that the impaired fear response is not due to a secondary effect of these sensory systems.

2. *Bbs1*$^{M390R/M390R}$ mice have normal short-term fear conditioning.

We tested short-term fear conditioning in BBS mice to assess if the long-term memory deficit is due to short-term memory impairment. To test for short-term fear conditioning, we used a 1-day fear conditioning paradigm (Fig 2A). Both the control mice (*Bbs1*$^{M390R/+}$ mice) and *Bbs1*$^{M390R/M390R}$ mice showed intact conditioning to shock (Fig 2B). In addition, there was no significant difference in short-term context memory between the control mice and *Bbs1*$^{M390R/M390R}$ mice (Fig 2C). These results are in contrast to the differences in long-term context memory, which showed impaired performance in *Bbs1*$^{M390R/M390R}$ mice compared to controls (Fig 1C). These findings indicated that BBS mice have specific impairments in long-term context fear conditioning.

3. Mice with postnatal deletion of *Bbs8* have impaired long-term context fear conditioning

We took advantage of another BBS mouse model to further explore the role of BBS genes (especially BBSome genes) in fear conditioning, specifically a tamoxifen inducible knock-out mouse model of BBS8 [36]. BBS8, like BBS1, is a component of the BBSome [11]. Using *Bbs8* tamoxifen inducible knock-out mice, we evaluated the temporal effects of BBS8 on fear conditioning (Fig 3A). For controls, we used littermates lacking *Cre.* Tamoxifen was administered to both groups of mice to control for possible effects of tamoxifen on behavior [37]. Following day 1 of fear conditioning, mice with *Bbs8* postnatally deleted, as well as control mice, were successfully conditioned to fear (Fig 3B). However, significant impairments in context but not cue fear conditioning were observed between conditional KO *Bbs8* mice and controls

(Fig 3C). These results are similar to the results for *Bbs1*$^{M390R/M390R}$ mice, indicating a role of the BBSome in mediating long-term context fear conditioning. Although, we observed differences in the acquisition curve of day 1 fear conditioning between conditional KO *Bbs8* mice and controls, no difference was found in immediate fear conditioning (Fig 3B and 3C). These results indicate that like *Bbs1*, *Bbs8* is involved in long-term context fear conditioning.

4. Mice with preferential deletion of *Bbs1* in the forebrain have impaired long-term context fear conditioning

The forebrain contains brain regions involved in fear conditioning including the amygdala and hippocampus[30]. To explore whether the absence of normal BBS1 function in the forebrain is responsible for the fear conditioning impairment observed in *Bbs1*$^{M390R/M390R}$ mice, we utilized a forebrain-specific *Bbs1* knock-out mouse line developed by crossing a *Bbs1*$^{flox/flox}$ conditional mouse line with a *Cre* line expressed in the forebrain (*Emx1-Cre* mice). The *Emx1-Cre* mice were generated and verified by Gorski et al. [38]. Using an Ai9 Cre reporter allele, we confirmed that the Cre is preferentially expressed in the forebrain (S4A and S4B Fig). We also confirmed that *Bbs1* is excised in the forebrain, but unexcised in the hindbrain of *Bbs1*$^{flox/flox}$, *Emx1-Cre*+ mice (S4C Fig), further confirming the specificity of *Cre* expression in *Emx1-Cre* mice.

Control mice (*Emx1-Cre, Bbs1*$^{+/+}$ mice*)* and forebrain specific *Bbs1* knockout mice (*Emx1-Cre*; *Bbs1*$^{flox/-}$ mice) were fear conditioned using a three-day fear conditioning paradigm (Fig 4A). Acquisition of conditioning to shock was intact for both control mice and forebrain specific *Bbs1* knockout mice (Fig 4B). However, forebrain specific *Bbs1* knockout mice showed impaired context fear conditioning compared to controls (Fig 4C). Cue fear conditioning was observed to be intact for both knockout and control mice. These results indicate that BBS1 in the forebrain is required for contextual memory.

5. *Bbs1*$^{M390R/M390R}$ mice do not have impaired long-term potentiation

Since *Bbs1*$^{M390R/M390R}$ mice have impaired context fear conditioning, which is hippocampus dependent [30], we investigated hippocampal function in *Bbs1*$^{M390R/M390R}$ mice. We evaluated long-term potentiation (LTP) in the CA1 region of the hippocampus because LTP is a neural correlate for long-term memory consolidation [39]. In addition, some mouse models with impaired context fear conditioning have impaired long-term potentiation (LTP) in CA1 of the hippocampus [32, 40, 41]. Despite the important role of LTP in fear conditioning, we did not observe a difference in LTP between control mice and *Bbs1*$^{M390R/M390R}$ mice in CA1 of the hippocampus (Fig 5A and 5B). These results suggest that the observed impaired learning arises from causes other than impaired LTP.

6. *Bbs1*$^{M390R/M390R}$ mice have decreased hippocampal neurogenesis

Next, we sought to identify a potential cause of the defective long-term fear conditioning observed in BBS mice, It has been recently reported that BBS patients have decreased hippocampal volume which is thought to be a result of impaired neurogenesis [42]. Due to the known role that cilia play in mediating cell proliferation and hippocampal volume in patients [43, 44], we hypothesized that defective hippocampal neurogenesis underlies the fear conditioning deficits in BBS mice. Therefore, we investigated hippocampal neurogenesis in *Bbs1*$^{M390R/M390R}$ mice.

To measure proliferation, we injected *Bbs1*$^{M390R/M390R}$ mice and control mice with BrdU, a thymidine analog that is incorporated into replicating DNA to label proliferating cells (Fig 5C and 5E). Following BrdU labeling, we found that both neonatal (P3) and young adult (P44) *Bbs1*$^{M390R/M390R}$ mice displayed significant reductions in BrdU+ cells in the hippocampal dentate gyrus compared to controls (Fig 5D, Fig

5F-5H). Moreover, young adult *Bbs1*$^{M390R/M390R}$ mice also showed fewer new neurons as determined by a reduced number of cells co-labeled for BrdU and Doublecortin, a marker for immature neurons(Fig 6B and 6D) [45].

The role of the observed impairments in hippocampal neurogenesis in long-term context fear conditioning of *Bbs1*$^{M390R/M390R}$ is unclear. To test the role of neurogenesis, we utilized a pharmacological modality to enhance hippocampal neurogenesis. Because impaired neurogenesis within the dentate gyrus is associated with long term memory deficits, we reasoned that rescue of impaired neurogenesis could improve fear conditioning impairments. To this end, we chose lithium due to its previous use as an agent to improve neurogenesis and hippocampal dependent memory [46-48].

We began by assessing the effects of lithium on hippocampal neurogenesis in *Bbs1*$^{M390R/M390R}$ mice and control mice. Young adult mice were treated with lithium or vehicle (water) for two weeks, and then brain tissues were harvested and stained for BrdU and Doublecortin (Fig 6A and 6B). Compared to vehicle treated mice, lithium treatment led to a 153% increase in the number of new neurons in the dentate gyrus of the hippocampus (Fig 6C and 6D).

7. Lithium treatment rescued long-term context fear conditioning in *Bbs1*$^{M390R/M390R}$ mice

We hypothesized that enhancing hippocampal neurogenesis using lithium treatment would rescue context which is hippocampus dependent [30]. To test the effects of lithium on fear conditioning, 4-5 week old mice were administered lithium or vehicle for two weeks (Fig 6E). The mice underwent fear conditioning using the three-day paradigm (Fig 6E-6G). As hypothesized, lithium treatment rescued the long-term context fear conditioning, but not long-term cue fear conditioning for *Bbs1*$^{M390R/M390R}$ mice (Fig 6G).

271 Taken together, these obserations suggest BBS genes play an important role in mediating hippocampal

272 neurogenesis and long-term context fear conditioning.

273

Discussion:

Intellectual disability (ID) is the most common neurodevelopmental disorder [1]. ID has limited pharmacological treatments, which is attributed to a limited understanding of the mechanisms involved. A large reason for the lack of mechanistic understanding is due to a lack of mouse models with ID as a primary phenotype. To overcome this hurdle, we explored the use of mouse models of the human disorder, Bardet-Biedl Syndrome (BBS) for the study of ID.

We showed that BBS mice have impaired context fear conditioning, indicating that BBS genes play a critical role in long-term memory. Our studies elucidated the spatial and temporal role of BBS gene function in fear memory. Using a conditional *Bbs1* knock-out mouse model, we demonstrated that BBS1 in the forebrain plays an important role in long-term fear memory. These findings are consistent with prior reports that cilia in the forebrain are involved in long-term fear memory[49]. In addition, the use of a novel tamoxifen inducible *Bbs8* knock-out mouse model demonstrated that BBS gene function is also critical during the post-natal consolidation of long-term fear memory.

Our work is in contrast to previous work using BBS mice to study their role in fear conditioning, which gave inconsistent results [50, 51]. This is partially explained by the use of different mouse strains and testing parameters. This previous work used *Bbs4* null mice on C57BL/6 [51] or FVB/NJ[50] backgrounds. In addition, these studies have noted a sex difference in BBS mice (*Bbs4* knock-out mice) with respect to fear conditioning, which we do not observe [51]. The discrepancies in findings may be due to differences in mouse strains or study design. Our study primarily used strains 129/SvEv and C57BL/6. We used a strong learning paradigm with five pairings of shocks, compared to three shock pairings[51] or two shock pairings[50]. BBS4 mice were evaluated in the previous study compared to BBS1M390R and BBS8 knock-out mice in the current study. Although BBS4, BBS1 and BBS8 are all components of the BBSome, it is possible that these proteins could have unique properties on fear memory.

Since BBS is a pleiotropic disorder, there are other factors that could explain the context fear conditioning impairment observed in mouse models of BBS. The *Bbs1*$^{M390R/M390R}$ mice have visual deficits [24], olfactory deficits [52], obesity [24] and hydrocephalus, which could globally affect fear conditioning. In order to control for these phenotypes, we used young adult mice prior to the onset of obesity and blindness. In addition, our BBS1 conditional knock-out mice are not blind nor obese and BBS8 conditional knock-out mice do not have hydrocephalus [19, 53], yet both models have impaired long-term context fear conditioning. We are not able to account for the olfactory deficit as a confounding factor. However, if these phenotypes underlie the observed fear conditioning deficits, *Bbs1*$^{M390R/M390R}$ mice would also display short-term (immediate) fear conditioning deficits in addition to long-term deficits, which we did not observe. Therefore, we conclude that the fear learning deficits observed are a primary phenotype due to the absence of BBS gene function.

Other mouse models demonstrate fear memory deficits similar to those we report in this study. For example, long-term context fear conditioning, but not short-term context fear conditioning, has been reported in mice with absent neuronal nitric oxide synthase [34], mice with inhibited protein synthesis [33], and in mice with PKA [32, 33] or MAP Kinase deficiencies [33]. While these mouse models have impaired long-term potentiation (LTP) in CA1 of the hippocampus, there are mouse models with impaired memory that have normal LTP [49, 54] as is the case with our *Bbs1*$^{M390R/M390R}$ mice.

The decreased hippocampal neurogenesis in *Bbs1*$^{M390R/M390R}$ mice is a novel finding that can explain the impaired fear context memory. Hippocampal neurogenesis is involved in hippocampus dependent learning, such as context fear conditioning. Impaired context fear conditioning has been reported in mice with genetic suppression of proliferation of GFAP expressing cells [55, 56] and Nestin expressing cells [57, 58]. Impaired fear context long-term memory has also been repoted in mice with suppressed

hippocampal neurogenesis through irradiation of the head [59] and ganciclovir treated mice [55], supporting our results using BBS mouse models.

We speculate that BBS proteins affect hippocampal neurogenesis because BBS is involved in ciliary receptor trafficking of the Smoothened Receptor [13, 60, 61], which is involved in in SHH signaling. SHH signaling is mediated by primary cilia [43]. Primary cilia are particularly enriched in the hippocampus [62]. Furthermore, SHH signaling has a proliferative effect on adult hippocampal progenitors *in vitro and in vivo* [63]. In addition, both primary cilia and smoothened receptors (hedgehog signaling) are required by adult neural stem cells [64]. The role of BBS in hippocampal proliferation may also be due to their involvement in tyrosine receptor kinase B (TrkB) receptor signaling [17]. Brain derived neurotrophic factor (BDNF) has been shown to increase neurogenesis through TrkB receptors [65, 66].

We investigated lithium as a treatment for the memory and neural deficits of $Bbs1^{M390R/M390R}$ mice. Lithium has been shown to improve learning and memory tasks in mouse models of cognitive disease including Fragile X syndrome[67], Down syndrome[48], and Alzheimer disease[46]. In addition, lithium treatment affects the morphology of primary cilia in the brain[68] and lithium has also been shown to increase hippocampal neurogenesis [46, 48, 69]. While lithium treatment of $Bbs1^{M390R/M390R}$ mice produced a robust effect on memory performance, lithium treatment produced a more modest response in hippocampal proliferation and neurogenesis. This suggests that a modest change in hippocampal proliferation and neurogenesis can produce a profound effect on memory. Consistent with these findings, a Danish study shows a correlation between lower incidence of dementia and long-term exposure to lithium in drinking water[70]. In addition, a study in China showed that low-dose lithium treatment improved cognitive performance in children with ID without major side effects[71]. Our results demonstrate the therapeutic potential of an FDA approved drug, lithium, for treating the cognitive and neural phenotypes of BBS patients.

It is possible that lithium has other neural effects contributing to the rescue of context fear conditioning. For example, lithium has been reported to alter dendritic spine density in the hippocampus [72] and to improve olfaction in mouse models of olfactory impairment [73, 74].

Further research is needed to explore factors involved in decreased hippocampal neurogenesis in *Bbs1*$^{M390R/M390R}$ mice. In our young adult mouse study, we observed a decrease in the number of BrdU+/Doublecortin+ cells in the hippocampus, indicating decreased neurogenesis. However, the apparent decrease in neurogenesis could be due to decreased proliferation, decreased differentiation and/or decreased. Any of these factors could be likely because BBS proteins are involved in the function of primary cilia, and primary cilia are involved in proliferation, differentiation [75] and survival[76].

There are alternative explanations for the cause of the impaired learning and memory in BBS mouse models. BBS proteins traffic other ciliary receptors that are involved in learning and memory. *Bbs4* knock-out mice [16] and *Bbs7* knock-out mice [77] accumulate dopamine 1 (D1) receptors in cilia. D1 receptors are involved in learning and memory[78, 79]. BBS proteins are also involved in trafficking of the somatostatin receptor 3 (SSTR3) [60] and melanin concentrating hormone receptor 1 (MCHR1) [15], both of which are involved in learning and memory [80, 81].

Our mouse model of a ciliopathy with ID robustly presented with impaired fear memory in context fear conditioning and decreased neurogenesis. In addition, our mouse model of BBS presented similarly to the mouse model of Fragile X Syndrome[82]. Fragile X syndrome is one of the most commonly inherited disorders for intellectual disability [83], and has recently been found to have defective cilia [84]. Overall, the findings presented here support the use of BBS mice as a model for ID and support the use of pro-neurogenic treatments as a possible treatment for ID.

377

Methods

Study Approval:

This research was conducted in strict accordance to the Guide for the Care and Use of Laboratory Animals, 8th edition, from the National Research Council. All mice were handled based on approved Institutional Animal Care and Use Committee (IACUC) protocols (#5061426 and #8072147) at the University of Iowa. Animals were housed in facilities, maintained by the Office of Animal Resources that adhere to IACUC recommendations. Mice were euthanized either by anesthesia induced by I.P injection of ketamine/xylazine followed by transcardiac perfusion, or carbon dioxide inhalation followed by cervical dislocation. Every effort was made to minimize suffering in the mice, and humane endpoints were stringently observed.

Animals

All mice were group housed on a set 12 hr light-dark cycle and given standard chow (LM-485; Teklab, Madison, WI, USA) and water ad libitum. Mice were generated at the University of Iowa Carver College of Medicine and all experiments were performed in accordance with the Institute for Animal Care and Use Committee at the University of Iowa. For all testing, we used young adult mice (1.5-3 month old mice), unless otherwise noted. The ages of mice were chosen to keep the weight and visual processing differences between *Bbs1*$^{M390R/M390R}$ and control mice to a minimal [24]. All testing was conducted during the light cycle, unless otherwise noted.

We used several strains of mice as listed below. Control mice were of the same genetic strains as the mice with which they were compared. We used male and female mice on a pure 129/SvEv genetic background for *Bbs1*$^{M390R/M390R}$ mice and littermate controls (*Bbs1*$^{+/+}$ and *Bbs1*$^{M390R/+}$). Heterozygote mice (*Bbs1*$^{M390R/+}$)

404 do not exhibit BBS phenotypes [24, 47], and are not significantly different in fear conditioning compared
405 to *Bbs1*$^{+/+}$ mice. To generate mice with preferential *Bbs1* deletion in the forebrain, we crossed *Bbs1*$^{flox/flox}$
406 mice (129/SvEv) [47] with *Emx1-Cre* knock-in mice (C57BL/6) (Jackson Laboratory, #005628). To
407 verify forebrain *Cre* expression, we crossed *Emx1-Cre* knock-in mice with the Ai9 *Cre* reporter line
408 *Gt(ROSA)26Sor*$^{tm9(CAG-tdTomato)Hze}$ (C57BL/6) (Jackson Laboratory #007909). We also used conditional
409 *Bbs8* knock-out mice (*Bbs8*$^{flox/flox}$, C57BL/6) [36] crossed with tamoxifen-inducible *Cre* recombinase
410 mice, B6.Cg-*Ndor1*$^{Tg(UBC-cre/ERT2)1Ejb}$/2J (Jackson Laboratory #008085).
411
412
413 **Tamoxifen-inducible excision of *Bbs8***
414
415 We postnatally excised *Bbs8* according to previously described procedures [36]. To induce Cre
416 expression, *Bbs8*$^{flox/flox}$ and *Bbs8*$^{flox/-}$; *UBC-Cre*^{ERT2}+ mice were injected subcutaneously with 40 μL of
417 tamoxifen (15 mg/mL in corn oil) on three separate days (P9, P12, and P15). *Bbs8*$^{flox/flox}$ and *Bbs8*$^{flox/-}$;
418 *UBC-Cre*^{ERT2}- mice injected with tamoxifen were the littermate controls. We assessed excision efficiency
419 as previously described [36]. The *Bbs8* tamoxifen inducible knock-out mice (*Bbs8*$^{flox/flox}$ and *Bbs8*$^{flox/-}$;
420 *UBC-Cre*^{ERT2}+) that were determined to have less than 90% excision were excluded from the research
421 study. This was decided as an exclusion criterion prior to conducting the study. No other mice were
422 excluded from the research study.
423
424
425 **Behavioral Testing**
426
427 All behavioral testing was conducted during the light cycle, unless otherwise noted.
428

Delay Fear Conditioning: For fear conditioning, mice were placed in a fear conditioning chamber with near-infrared video. Freezing was scored with the VideoFreeze software (Med Associates, St. Albans, VT, USA). Fear conditioning can distinguish short-term context memory from long-term context memory based on when context fear conditioning is tested (short-term is 1 hour after conditioning, and long-term is ≥24 hours after conditioning) [32-34]. A 3-day protocol was used to assess both long-term cue and contextual fear conditioning.

- On the first day of fear conditioning, a 20-second tone (75 dB) was played, which co-terminated with a 1-second foot shock (0.75 mA). The tone-shock pairings occurred five times, with the shocks at 3:20m, 5:40m, 8m, 10:20m and 12:40m. For the acquisition curve figure, the freezing data was reported as the percent time the mouse was immobile for each one-minute bout. In addition, the training in day 1 fear conditioning was measured as:
    - Immediate fear conditioning = freezing time (%) just after conditioning (last minute) - the freezing time (%) just before conditioning (first three minutes)
- On the second day, to test cue fear conditioning, mice were tested in a novel context in which floor texture, odor, and shape of the chamber had been altered. After 3 minutes in the chamber, a 3-minute tone (75 dB) was delivered, followed by an additional 4 minutes without the tone. The cue fear conditioning was measured as:
    - Cue fear conditioning = freezing time (%) during the tone on day 2 – freezing time (%) before the tone on day 2
- On the third day, to test contextual fear conditioning, the chamber was set back to the original training context. Mice were place in the chamber for 5 minutes. The context fear conditioning was measured as:
    - Context fear conditioning = freezing time (%) on day 3 - freezing time (%) just before conditioning (first three minutes of day 1).

One day fear conditioning: The acquisition protocol for three-day fear conditioning was used for the one day fear conditioning protocol. After the acquisition phase, mice were placed back into their home cage. One hour after the fear conditioning, mice were placed back into the original training chamber, and recorded for five minutes. The short-term context fear conditioning was measured as the difference of the freezing time (%) just before conditioning (first three minutes of day 1) and during the context on day 1 (one hour after fear conditioning).

Preyer Reflex: The Preyer reflex is the startle response to auditory stimuli. Mice were given an auditory stimulus (hand clap) in their home cage. A positive sign was noted if the mouse had a rapid movement of the whole body after the auditory stimulus.

Circling Behavior: Circling behavior is noted in animal models of deafness [85]. Mice were observed for 5 minutes in their home cage for circling behavior. A positive circling behavior was noted if the mouse tightly circled around itself more than two times.

Auditory Brainstem Response

The auditory brainstem response (ABR) test provides information about the auditory sensitivity of the subject. The ABR test was conducted on 2-month old control mice (n=3) and *Bbs1*$^{M390R/M390R}$ mice (n=4). The experimenter was masked to the genotype. The ABR test were conducted as previously described [86]. Briefly, clicks and tone-bursts were delivered to the testing ear through a plastic acoustic tube in a sound attenuated room. ABRs were measured using an Etymotic Research ER10B+ probe microphone (Etymotic Research, Elk Grove, IL, USA) coupled to two Tucker-Davis Technologies MF1 multi-field magnetic speakers (Tucker-Davis Technologies, Alachua, FL, USA). Click and tone-burst stimuli were presented and recorded using custom software running on a PC connected to a 24-bit external sound card (Motu UltraLite mk3, Cambridge MA, USA). A custom-built differential amplifier with a gain of 1,000

dB amplified acoustic ABR responses. Output was passed through 6-pole Butterworth high-pass (100 Hz) and low-pass (3 kHz) filters and then to a 16-bit analog-to-digital converter (100,000 sample/s). The tone bursts were 3 ms in length, in addition to 1 ms onset and offset ramps (raised cosine shape) centered at 4, 8, 16, 24, and 32 kHz. Responses were recorded using standard signal-averaging techniques for 500 or 1000 sweeps. Hearing thresholds (db SPL) were determined by decreasing the sound intensity by 5 and/or 10 db decrements and recording the lowest sound intensity level resulting in a recognizable and reproducible ABR response wave pattern. Maximum ABR thresholds were capped at 100 db SPL.

BrdU injections

For early postnatal time points, mice were injected intraperitoneally with 300mg/kg Bromodeoxyuridine (BrdU, Sigma, St. Louis, Missouri) and sacrificed 4 hours after the injection. For later postnatal time points, mice were injected intraperitoneally with 50mg/kg BrdU twice a day for five days, and sacrificed ten days later.

Lithium Treatment

We treated mice with 45mmol lithium chloride (Sigma) in drinking water starting at four to five weeks of age for 2 weeks. Mice were group-housed for lithium treatment and group-housed for vehicle (water) treatment. Littermate controls were group-housed.

Tissue collections and histology

For early postnatal tissue, fresh brain tissues were collected and embedded in Optimal Cutting Temperature compound (OCT, Tissue Tek, Sakura Finetek). Eight µm sections were cut on a cryostat.

For late postnatal time points, mice were anesthetized by intraperitoneal injection of Ketamine (17.5 mg/cc)/Xylazine (2.5 mg/cc) at 100 μL/20 gram body weight, and transcardially perfused with 4% paraformaldehyde in phosphate-buffered saline (PBS). The brain and eyes were removed and post-fixed overnight at 4°C with 4% paraformaldehyde in PBS, followed by more than 24 hours of immersion in 30% sucrose in PBS. Tissues were then embedded in OCT (Tissue Tek, Sakura Finetek). 20 μm sections were cut on a cryostat.

Immunohistochemistry

Tissue sections were directly placed on positively charged microscope slides (Globe Scientific). Tissue sections were fluorescently immunostained for the following markers: anti-tdtomato: 1:500 rabbit polyclonal anti-DsRed (Living Colors), immature neuronal marker anti-Doublecortin (1:500, abcam) proliferative marker anti-BrdU (1:200, Abcam). The AlexaFluor tagged secondary antibodies used were Alexa488 (green), Alexa568 (red), and Alexa633 (far red) (Molecular Probes). Antigen retrieval was used for neuronal markers (50 mMol Tris HCl, 45 minutes at 80 °C) and BrdU marker (2N HCl, 0.1% triton, 30 minutes in 37°C)

In preparation for staining, slides with sections were placed in 50 mM Tris HCl for 45 minutes at 80°C. After slides were cooled, slides were incubated in 2N HCl (0.1% Triton) at 37°C for 30 minutes and rinsed in 0.1 M boric acid (pH 8.5) at room temperature for 10 minutes. Sections were then rinsed in PBST (0.2% Triton X-100/ PBS), blocked for one hour with block solution (2% bovine serum in PBS/0.1% Triton X-100), and incubated overnight with anti-BrdU antibody and anti-Hu antibody in serum solution (1% bovine serum in PBS/0.1% Triton X-100) at 4°C. Sections were washed in PBST, incubated with secondary antibodies in serum solution at RT for 2 hours, washed in PBST, counterstained with DAPI, and cover slipped with Vectashield© antifade mounting medium (Vector Laboratories).

Cell quantification

Tissue sections used for BrdU quantification were imaged using an inverted fluorescent microscope (Olympus IX71). Exposure was kept constant for each channel within experiments. Four to six representative dentate gryi from coronal sections were counted per mouse subject. The number of BrdU+ cells were counted within the dentate gyrus of a 20x image (Figure 3C). BrdU is a maker for proliferating cells. The BrdU+ cell counts were standardized to the volume of dentate gyrus tissue in the image (mm^3). Volume was determined by measuring the area of the dentate gyrus on ImageJ and multiplying the area by the thickness of the tissue. For analysis of neurogenesis, Doublecortin+BrdU+ and BrdU+ cell within the dentate gyrus were counted. Doublecortin is a marker for immature neurons [45]. The tissue sections used for quantification were imaged using confocal microscopy (SP8 confocal microscope, Leica). To determine the frequency of BrdU+ cells expressing DCX, dual fluorescence-labeled sections were examined by confocal microscopy using a 20x objective (Figure 3F, S6). Sections were scored for single or double labeling by manual examination of optical slices. Cells were manually counted for double labeling when DCX labeling was unambiguously associated with a BrdU+ nucleus. Cells were spot-checked in all three dimensions by Z-stack using a 20x objective. In all cases, the observer was masked to the treatment and genotypes.

Comprehensive Lab Animal Monitoring System

For analysis of whole animal activity levels and sleep behavior, *Bbs1*$^{M390R/M390R}$ mice (n=7) and control mice (n=9) were placed in a Comprehensive Lab Animal Monitoring System (CLAMS; Columbus Instruments, Columbus, OH, USA). CLAMS is an open circuit system that directly measures various parameters over a 72 hour period including movement, sleep behavior, food intake, VO2, VCO2, and heat production. Mice were weighed before the CLAMS recording. Mice were individually housed in

Plexiglas cage chambers that were kept at 24°C under a 12:12 hour light-dark cycle. The chamber had 0.6 liters of air passed per minute. Movement (activity) was measured by XY laser beam interruption, and sleep behavior was measured as minimum movement for four minutes or longer. Food consumption was monitored by electronic scales. For measuring the O2 and CO2, the gas content of the exhaust air from each chamber was compared with the gas content of the ambient air sample. The V□O2 and V□CO2 measurements were normalized to mouse body weight. The following parameters were calculated as followed: RER = V□CO2/V□O2, heat production = 1.232*VCO2+3.815*VO2. CLAMS were performed at the University of Iowa Fraternal Order of Eagles Diabetes Research Center Metabolic Phenotyping Core.

Slice preparation and electrophysiology

Hippocampal slices from group-housed, naive 2-months old *Bbs1*$^{M390R/M390R}$ mice (n=4) and control mice (n=4) were prepared as previously described [87].First, tissue brain blocks were affixed to the cutting stage, submersed in cutting solution, and transversely sectioned at 400 μm on a Vibratome 1000 Plus (Vibratome, St. Louis, MO). After bisecting into hemispheres, slices were transferred to a holding chamber containing artificial cerebrospinal fluid (aCSF). After 30 minutes, the holding chamber was removed from the water bath and held at RT (22°C) for the remainder of the experiment.

To record field excitatory post-synaptic potentials (fEPSP), aCSF-filled borosilicate electrodes (Corning #0010 glass, resistance <1 MΩ) were positioned in the stratum radiatum of area CA1. Synaptic responses were evoked by stimulation of Schaffer collaterals with bipolar tungsten electrodes (0.1 MΩ, parylene coated; World Precision Instruments, Sarasota, FL). Signals were amplified (AxoClamp 900A Amplifier, Axon Instruments, Foster City, CA), filtered at 1 kHz, digitally-sampled at 10 kHz (Axon Digidata 1440), and stored for offline analysis in Clampfit 10 (Molecular Devices, San Jose, CA).

An input-output curve (initial slope of fEPSP plotted against stimulus intensity) for assessment of basal synaptic transmission was first generated by delivering pulses of 0.2 ms duration every 15 s at increasing stimulation intensities to elicit synaptic responses. Stimulation intensity was then adjusted to yield 40 - 60% of the maximal fEPSP amplitude. The input/output curve is primarily used to calibrate the setting for LTP of the tissue, along with assessing the viability of the tissue.

After acquiring stable baseline responses for 15 minutes, LTP was induced by a theta-burst stimulation protocol consisting of 12 bursts of 4 pulses at 100 Hz. Synaptic responses were sampled every 15 s for 1 h after induction. For analysis, the initial slope of each fEPSP was normalized to the average baseline slope. Time-matched, normalized slopes were then averaged among slices from animals of the same genotype for comparison and plotted as an average of four consecutive responses (*i.e.*, responses sampled over 1 minute). Slices with maximal fEPSPs of less than 0.5 mV, disproportionately large fiber volleys, substantial changes in fiber volley amplitude during LTP recordings, or unstable synaptic responses during baseline or LTP recordings were excluded.

Statistical Analysis:

Statistical analyses were performed using GraphPad Prism 8.0 (GraphPad Software, San Diego, CA). For comparison of two groups, we ran a two-tailed Welch's t-test. The Welch's t-test is recommended over the Student t-test because Welch's t-test performs better when the sample sizes and variances are unequal between groups, and gives similar results when sample sizes and variances are equal [88, 89]. Preliminary tests of equality of variances to determine t-tests are not recommended since it impairs the validity of the Welch's t-test [90]. For data that appear skewed, we also ran a Mann-Whitney-Wilcoxon Test. For multiple comparisons, we ran multiple t-tests (analyzed each row individually and did not assume consistent standard deviations) corrected for multiple comparisons using the Holm-Sidak method. A two-way ANOVA was used for comparisons of multiple groups with two different independent variables. We then ran a Sidak post-hoc analysis for the relevant data. A three-way ANOVA was used for comparison of

609 multiple groups with three different independent variables. Graphs were generated on GraphPad Prism
610 8.0. Data are presented as mean with the error bars indicating standard error of means (unless otherwise
611 noted).
612
613
614 **Author Contributions**
615
616 Conceived and designed the experiments: TP, CSC, RT, AP, JW, VCS, HS, and QZ. Performed the
617 experiments: TP, TV, CSC, CS, YH, CCC, and RG. Analyzed the data: TP, CSC, SCH, NM, CCC, RG,
618 RT, VCS, and KW. Contributed reagents/materials/analysis tools: CSC, SCH, NM, YH, AP, and JW.
619 Wrote the paper: TP, CSC, HS, QZ, RT, JW and VCS.
620
621 **Acknowledgements**
622
623 We thank Valerie Bouffard and Janelle Garrison for the animal husbandry and genotyping. We thank
624 Chantal Allamargot and Kathy Walters, in the Central Microscopy Research Facility at the University of
625 Iowa, for technical assistance in microscopy. We thank Paul Ranum and Richard Smith for their technical
626 assistance with the Auditory Brainstem Response. We want to acknowledge Jamie Soto of the Metabolic
627 Phenotype Core at the University of Iowa, for her technical help with CLAMS. We thank Hamza Farooq
628 for drawing Figure 1a. We thank AJ Chowdhury for assisting with editing of the manuscript. We would
629 also like to acknowledge Denise Harder for her administrative support.
630
631

References

1. Bavley CC, Rice RC, Fischer DK, Fakira AK, Byrne M, Kosovsky M, et al. Rescue of Learning and Memory Deficits in the Human Nonsyndromic Intellectual Disability Cereblon Knock-Out Mouse Model by Targeting the AMP-Activated Protein Kinase–mTORC1 Translational Pathway. The Journal of Neuroscience. 2018;38(11):2780-95.
2. Maulik PK, Mascarenhas MN, Mathers CD, Dua T, Saxena S. Prevalence of intellectual disability: A meta-analysis of population-based studies. Research in Developmental Disabilities. 2011;32(2):419-36.
3. von Wilamowitz-Moellendorff A, Hunter RW, García-Rocha M, Kang L, López-Soldado I, Lantier L, et al. Glucose-6-phosphate-mediated activation of liver glycogen synthase plays a key role in hepatic glycogen synthesis. Diabetes. 2013;62(12):4070-82. Epub 2013/08/29.
4. Picker JD, Walsh CA. New innovations: therapeutic opportunities for intellectual disabilities. Annals of neurology. 2013;74(3):382-90. Epub 2013/09/17.
5. Scorza CA, Cavalheiro EA. Animal models of intellectual disability: towards a translational approach. Clinics (Sao Paulo, Brazil). 2011;66 Suppl 1(Suppl 1):55-63.
6. Park SM, Jang HJ, Lee JH. Roles of Primary Cilia in the Developing Brain. Frontiers in Cellular Neuroscience. 2019;13(218).
7. Oh EC, Vasanth S, Katsanis N. Metabolic regulation and energy homeostasis through the primary Cilium. Cell metabolism. 2015;21(1):21-31. Epub 12/24.
8. Beales PL, Elcioglu N, Woolf AS, Parker D, Flinter FA. New criteria for improved diagnosis of Bardet-Biedl syndrome: results of a population survey. Journal of medical genetics. 1999;36(6):437-46. Epub 2000/06/30.
9. Forsythe E, Beales PL. Bardet-Biedl syndrome. European journal of human genetics : EJHG. 2013;21(1):8-13.
10. Sheffield V, Zhang Q, Heon E, drack AV, Stone AEL, Carmi R. Epstein's Inborn Errors of Development: The Molecular Basis of Clinical Disorders of Morphogenesis: Oxford University Press; 2016.
11. Nachury MV, Loktev AV, Zhang Q, Westlake CJ, Peranen J, Merdes A, et al. A core complex of BBS proteins cooperates with the GTPase Rab8 to promote ciliary membrane biogenesis. Cell. 2007;129(6):1201-13. Epub 2007/06/19.
12. Loktev AV, Zhang Q, Beck JS, Searby CC, Scheetz TE, Bazan JF, et al. A BBSome subunit links ciliogenesis, microtubule stability, and acetylation. Dev Cell. 2008;15(6):854-65. Epub 2008/12/17.
13. Zhang Q, Seo S, Bugge K, Stone EM, Sheffield VC. BBS proteins interact genetically with the IFT pathway to influence SHH-related phenotypes. Human Molecular Genetics. 2012;21(9):1945-53.
14. Loktev Alexander V, Jackson Peter K. Neuropeptide Y Family Receptors Traffic via the Bardet-Biedl Syndrome Pathway to Signal in Neuronal Primary Cilia. Cell Reports. 2013;5(5):1316-29.
15. Berbari NF, Lewis JS, Bishop GA, Askwith CC, Mykytyn K. Bardet-Biedl syndrome proteins are required for the localization of G protein-coupled receptors to primary cilia. Proc Natl Acad Sci USA. 2008;105.
16. Domire JS, Green JA, Lee KG, Johnson AD, Askwith CC, Mykytyn K. Dopamine receptor 1 localizes to neuronal cilia in a dynamic process that requires the Bardet-Biedl syndrome proteins. Cellular and molecular life sciences : CMLS. 2011;68(17):2951-60. Epub 2010/12/15.
17. Leitch CC, Zaghloul NA. BBS4 Is Necessary for Ciliary Localization of TrkB Receptor and Activation by BDNF. PLOS ONE. 2014;9(5):e98687.
18. Seo S, Baye LM, Schulz NP, Beck JS, Zhang Q, Slusarski DC, et al. BBS6, BBS10, and BBS12 form a complex with CCT/TRiC family chaperonins and mediate BBSome assembly. Proceedings of the National Academy of Sciences. 2010;107(4):1488-93.
19. Zhang Q, Nishimura D, Seo S, Vogel T, Morgan DA, Searby C, et al. Bardet-Biedl syndrome 3 (Bbs3) knockout mouse model reveals common BBS-associated phenotypes and Bbs3 unique

phenotypes. Proceedings of the National Academy of Sciences of the United States of America. 2011;108(51):20678-83. Epub 2011/12/06.
20. Weihbrecht K, Goar WA, Pak T, Garrison JE, DeLuca AP, Stone EM, et al. Keeping an Eye on Bardet-Biedl Syndrome: A Comprehensive Review of the Role of Bardet-Biedl Syndrome Genes in the Eye. Medical research archives. 2017;5(9):10.18103/mra.v5i9.1526.
21. Huangfu D, Liu A, Rakeman AS, Murcia NS, Niswander L, Anderson KV. Hedgehog signalling in the mouse requires intraflagellar transport proteins. Nature. 2003;426.
22. Liu A, Wang B, Niswander LA. Mouse intraflagellar transport proteins regulate both the activator and repressor functions of Gli transcription factors. Development (Cambridge, England). 2005;132.
23. Cortellino S, Wang C, Wang B, Bassi MR, Caretti E, Champeval D, et al. Defective ciliogenesis, embryonic lethality and severe impairment of the Sonic Hedgehog pathway caused by inactivation of the mouse complex A intraflagellar transport gene Ift122/Wdr10, partially overlapping with the DNA repair gene Med1/Mbd4. Developmental biology. 2009;325(1):225-37. Epub 10/29.
24. Davis RE, Swiderski RE, Rahmouni K, Nishimura DY, Mullins RF, Agassandian K, et al. A knockin mouse model of the Bardet-Biedl syndrome 1 M390R mutation has cilia defects, ventriculomegaly, retinopathy, and obesity. Proceedings of the National Academy of Sciences of the United States of America. 2007;104(49):19422-7. Epub 2007/11/23.
25. Baker K, Northam GB, Chong WK, Banks T, Beales P, Baldeweg T. Neocortical and hippocampal volume loss in a human ciliopathy: A quantitative MRI study in Bardet–Biedl syndrome. American Journal of Medical Genetics Part A. 2011;155(1):1-8.
26. Crawley JN. What's Wrong With My Mouse?: Behavioral Phenotyping of Transgenic and Knockout Mice: John Wiley & Sons, Inc.; 2006. Available from: https://onlinelibrary.wiley.com/doi/book/10.1002/0470119055.
27. Murru L, Vezzoli E, Longatti A, Ponzoni L, Falqui A, Folci A, et al. Pharmacological Modulation of AMPAR Rescues Intellectual Disability-Like Phenotype in Tm4sf2-/y Mice. Cerebral cortex (New York, NY : 1991). 2017;27(11):5369-84. Epub 2017/10/03.
28. Rajadhyaksha AM, Ra S, Kishinevsky S, Lee AS, Romanienko P, DuBoff M, et al. Behavioral characterization of cereblon forebrain-specific conditional null mice: A model for human non-syndromic intellectual disability. Behavioural brain research. 2012;226(2):428-34.
29. Matzel LD, Han YR, Grossman H, Karnik MS, Patel D, Scott N, et al. Individual Differences in the Expression of a “General” Learning Ability in Mice. The Journal of Neuroscience. 2003;23(16):6423-33.
30. Phillips RG, LeDoux JE. Differential contribution of amygdala and hippocampus to cued and contextual fear conditioning. Behavioral neuroscience. 1992;106(2):274-85. Epub 1992/04/01.
31. Johansen Joshua P, Cain Christopher K, Ostroff Linnaea E, LeDoux Joseph E. Molecular Mechanisms of Fear Learning and Memory. Cell. 2011;147(3):509-24.
32. Abel T, Nguyen PV, Barad M, Deuel TA, Kandel ER, Bourtchouladze R. Genetic demonstration of a role for PKA in the late phase of LTP and in hippocampus-based long-term memory. Cell. 1997;88(5):615-26. Epub 1997/03/07.
33. Schafe GE, Atkins CM, Swank MW, Bauer EP, Sweatt JD, LeDoux JE. Activation of ERK/MAP Kinase in the Amygdala Is Required for Memory Consolidation of Pavlovian Fear Conditioning. The Journal of Neuroscience. 2000;20(21):8177-87.
34. Kelley JB, Balda MA, Anderson KL, Itzhak Y. Impairments in fear conditioning in mice lacking the nNOS gene. Learning & memory (Cold Spring Harbor, NY). 2009;16(6):371-8.
35. Curzon P, Rustay N, Browman K. Methods of Behavior Analysis in Neuroscience. Boca Raton (FL): CRC Press/Taylor & Francis; 2009. Available from: https://www.ncbi.nlm.nih.gov/books/NBK5223/.
36. Hsu Y, Garrison JE, Kim G, Schmitz AR, Searby CC, Zhang Q, et al. BBSome function is required for both the morphogenesis and maintenance of the photoreceptor outer segment. PLoS genetics. 2017;13(10):e1007057.

731 37. Li X, Du ZJ, Chen MQ, Chen JJ, Liang ZM, Ding XT, et al. The effects of tamoxifen on mouse
732 behavior. Genes Brain Behav. 2020;19(4):e12620. Epub 2019/10/28.
733 38. Gorski JA, Talley T, Qiu M, Puelles L, Rubenstein JLR, Jones KR. Cortical Excitatory Neurons
734 and Glia, But Not GABAergic Neurons, Are Produced in the Emx1-Expressing Lineage. The Journal of
735 Neuroscience. 2002;22(15):6309-14.
736 39. Cooke SF, Bliss TVP. Plasticity in the human central nervous system. Brain : a journal of
737 neurology. 2006;129(7):1659-73.
738 40. Bourtchuladze R, Frenguelli B, Blendy J, Cioffi D, Schutz G, Silva AJ. Deficient long-term
739 memory in mice with a targeted mutation of the cAMP-responsive element-binding protein. Cell.
740 1994;79(1):59-68.
741 41. Xie C-W, Sayah D, Chen Q-S, Wei W-Z, Smith D, Liu X. Deficient long-term memory and long-
742 lasting long-term potentiation in mice with a targeted deletion of neurotrophin-4 gene. Proceedings of the
743 National Academy of Sciences. 2000;97(14):8116-21.
744 42. Baker K, Northam GB, Chong WK, Banks T, Beales P, Baldeweg T. Neocortical and
745 hippocampal volume loss in a human ciliopathy: A quantitative MRI study in Bardet-Biedl syndrome.
746 American journal of medical genetics Part A. 2011;155a(1):1-8. Epub 2011/01/05.
747 43. Breunig JJ, Sarkisian MR, Arellano JI, Morozov YM, Ayoub AE, Sojitra S, et al. Primary cilia
748 regulate hippocampal neurogenesis by mediating sonic hedgehog signaling. Proceedings of the National
749 Academy of Sciences of the United States of America. 2008;105(35):13127-32. Epub 2008/08/30.
750 44. Amador-Arjona A, Elliott J, Miller A, Ginbey A, Pazour GJ, Enikolopov G, et al. Primary Cilia
751 Regulate Proliferation of Amplifying Progenitors in Adult Hippocampus: Implications for Learning and
752 Memory. The Journal of Neuroscience. 2011;31(27):9933-44.
753 45. Brown JP, Couillard-Després S, Cooper-Kuhn CM, Winkler J, Aigner L, Kuhn HG. Transient
754 expression of doublecortin during adult neurogenesis. The Journal of comparative neurology.
755 2003;467(1):1-10. Epub 2003/10/24.
756 46. Fiorentini A, Rosi MC, Grossi C, Luccarini I, Casamenti F. Lithium Improves Hippocampal
757 Neurogenesis, Neuropathology and Cognitive Functions in APP Mutant Mice. PLOS ONE.
758 2010;5(12):e14382.
759 47. Carter CS, Vogel TW, Zhang Q, Seo S, Swiderski RE, Moninger TO, et al. Abnormal
760 development of NG2+PDGFR-α+ neural progenitor cells leads to neonatal hydrocephalus in a ciliopathy
761 mouse model. Nature Medicine. 2012;18:1797.
762 48. Bianchi P, Ciani E, Contestabile A, Guidi S, Bartesaghi R. Lithium Restores Neurogenesis in the
763 Subventricular Zone of the Ts65Dn Mouse, a Model for Down Syndrome. Brain Pathology.
764 2010;20(1):106-18.
765 49. Berbari NF, Malarkey EB, Yazdi SM, McNair AD, Kippe JM, Croyle MJ, et al. Hippocampal and
766 cortical primary cilia are required for aversive memory in mice. PLoS One. 2014;9(9):e106576. Epub
767 2014/09/04.
768 50. Eichers ER, Abd-El-Barr MM, Paylor R, Lewis RA, Bi W, Lin X, et al. Phenotypic
769 characterization of Bbs4 null mice reveals age-dependent penetrance and variable expressivity. Hum
770 Genet. 2006;120(2):211-26.
771 51. Haq N, Schmidt-Hieber C, Sialana FJ, Ciani L, Heller JP, Stewart M, et al. Loss of Bardet-Biedl
772 syndrome proteins causes synaptic aberrations in principal neurons. PLOS Biology.
773 2019;17(9):e3000414.
774 52. Williams CL, Uytingco CR, Green WW, McIntyre JC, Ukhanov K, Zimmerman AD, et al. Gene
775 Therapeutic Reversal of Peripheral Olfactory Impairment in Bardet-Biedl Syndrome. Molecular therapy :
776 the journal of the American Society of Gene Therapy. 2017;25(4):904-16. Epub 02/22.
777 53. Singh M, Garrison JE, Wang K, Sheffield VC. Absence of BBSome function leads to astrocyte
778 reactivity in the brain. Molecular brain. 2019;12(1):48-.
779 54. Fragkouli A, Hearn C, Errington M, Cooke S, Grigoriou M, Bliss T, et al. Loss of forebrain
780 cholinergic neurons and impairment in spatial learning and memory in LHX7-deficient mice. The
781 European journal of neuroscience. 2005;21(11):2923-38. Epub 2005/06/28.

55. Saxe MD, Battaglia F, Wang J-W, Malleret G, David DJ, Monckton JE, et al. Ablation of hippocampal neurogenesis impairs contextual fear conditioning and synaptic plasticity in the dentate gyrus. Proceedings of the National Academy of Sciences. 2006;103(46):17501-6.
56. Denny CA, Burghardt NS, Schachter DM, Hen R, Drew MR. 4- to 6-week-old adult-born hippocampal neurons influence novelty-evoked exploration and contextual fear conditioning. Hippocampus. 2012;22(5):1188-201. Epub 2011/07/09.
57. Imayoshi I, Sakamoto M, Ohtsuka T, Takao K, Miyakawa T, Yamaguchi M, et al. Roles of continuous neurogenesis in the structural and functional integrity of the adult forebrain. Nature neuroscience. 2008;11(10):1153-61. Epub 2008/09/02.
58. Deng W, Saxe MD, Gallina IS, Gage FH. Adult-born hippocampal dentate granule cells undergoing maturation modulate learning and memory in the brain. The Journal of neuroscience : the official journal of the Society for Neuroscience. 2009;29(43):13532-42. Epub 2009/10/30.
59. Winocur G, Wojtowicz JM, Sekeres M, Snyder JS, Wang S. Inhibition of neurogenesis interferes with hippocampus-dependent memory function. Hippocampus. 2006;16(3):296-304. Epub 2006/01/18.
60. Ye F, Nager AR, Nachury MV. BBSome trains remove activated GPCRs from cilia by enabling passage through the transition zone. The Journal of Cell Biology. 2018.
61. Nozaki S, Katoh Y, Kobayashi T, Nakayama K. BBS1 is involved in retrograde trafficking of ciliary GPCRs in the context of the BBSome complex. PLoS ONE. 2018;13(3):e0195005.
62. Bishop GA, Berbari NF, Lewis J, Mykytyn K. Type III adenylyl cyclase localizes to primary cilia throughout the adult mouse brain. The Journal of comparative neurology. 2007;505(5):562-71. Epub 2007/10/11.
63. Lai K, Kaspar BK, Gage FH, Schaffer DV. Sonic hedgehog regulates adult neural progenitor proliferation in vitro and in vivo. Nature neuroscience. 2003;6(1):21-7. Epub 2002/12/07.
64. Han YG, Spassky N, Romaguera-Ros M, Garcia-Verdugo JM, Aguilar A, Schneider-Maunoury S, et al. Hedgehog signaling and primary cilia are required for the formation of adult neural stem cells. Nature neuroscience. 2008;11(3):277-84. Epub 2008/02/26.
65. Li Y, Luikart BW, Birnbaum S, Chen J, Kwon CH, Kernie SG, et al. TrkB regulates hippocampal neurogenesis and governs sensitivity to antidepressive treatment. Neuron. 2008;59(3):399-412. Epub 2008/08/15.
66. Islam O, Loo TX, Heese K. Brain-derived neurotrophic factor (BDNF) has proliferative effects on neural stem cells through the truncated TRK-B receptor, MAP kinase, AKT, and STAT-3 signaling pathways. Current neurovascular research. 2009;6(1):42-53. Epub 2009/04/10.
67. King MK, Jope RS. Lithium treatment alleviates impaired cognition in a mouse model of fragile X syndrome. Genes, Brain and Behavior. 2013;12(7):723-31.
68. Miyoshi K, Kasahara K, Miyazaki I, Asanuma M. Lithium treatment elongates primary cilia in the mouse brain and in cultured cells. Biochem Biophys Res Commun. 2009;388(4):757-62. Epub 2009/08/26.
69. Chen G, Rajkowska G, Du F, Seraji-Bozorgzad N, Manji HK. Enhancement of hippocampal neurogenesis by lithium. Journal of neurochemistry. 2000;75(4):1729-34. Epub 2000/09/15.
70. Kessing LV, Gerds TA, Knudsen NN, Jørgensen LF, Kristiansen SM, Voutchkova D, et al. Association of Lithium in Drinking Water With the Incidence of Dementia. JAMA Psychiatry. 2017;74(10):1005-10.
71. Yuan J, Song J, Zhu D, Sun E, Xia L, Zhang X, et al. Lithium Treatment Is Safe in Children With Intellectual Disability. Frontiers in molecular neuroscience. 2018;11:425-.
72. Shim SS, Hammonds MD, Mervis RF. Four weeks lithium treatment alters neuronal dendrites in the rat hippocampus. International Journal of Neuropsychopharmacology. 2013;16(6):1373-82.
73. Castro AA, Ghisoni K, Latini A, Quevedo J, Tasca CI, Prediger RD. Lithium and valproate prevent olfactory discrimination and short-term memory impairments in the intranasal 1-methyl-4-phenyl-1,2,3,6-tetrahydropyridine (MPTP) rat model of Parkinson's disease. Behavioural brain research. 2012;229(1):208-15. Epub 2012/01/24.

832 74. Guidi S, Bianchi P, Stagni F, Giacomini A, Emili M, Trazzi S, et al. Lithium Restores Age-
833 related Olfactory Impairment in the Ts65Dn Mouse Model of Down Syndrome. CNS & neurological
834 disorders drug targets. 2017;16(7):812-9. Epub 2016/08/05.
835 75. Irigoín F, Badano JL. Keeping the balance between proliferation and differentiation: the primary
836 cilium. Current genomics. 2011;12(4):285-97.
837 76. Bowie E, Goetz SC. TTBK2 and primary cilia are essential for the connectivity and survival of
838 cerebellar Purkinje neurons. eLife. 2020;9:e51166.
839 77. Zhang Q, Nishimura D, Vogel T, Shao J, Swiderski R, Yin T, et al. BBS7 is required for
840 BBSome formation and its absence in mice results in Bardet-Biedl syndrome phenotypes and selective
841 abnormalities in membrane protein trafficking. Journal of cell science. 2013;126(11):2372-80.
842 78. El-Ghundi M, Fletcher PJ, Drago J, Sibley DR, O'Dowd BF, George SR. Spatial learning deficit
843 in dopamine D(1) receptor knockout mice. European journal of pharmacology. 1999;383(2):95-106. Epub
844 1999/12/11.
845 79. Sarinana J, Kitamura T, Kunzler P, Sultzman L, Tonegawa S. Differential roles of the dopamine
846 1-class receptors, D1R and D5R, in hippocampal dependent memory. Proceedings of the National
847 Academy of Sciences of the United States of America. 2014;111(22):8245-50. Epub 2014/05/21.
848 80. Einstein EB, Patterson CA, Hon BJ, Regan KA, Reddi J, Melnikoff DE, et al. Somatostatin
849 signaling in neuronal cilia is critical for object recognition memory. The Journal of neuroscience : the
850 official journal of the Society for Neuroscience. 2010;30(12):4306-14. Epub 2010/03/26.
851 81. Adamantidis A, Thomas E, Foidart A, Tyhon A, Coumans B, Minet A, et al. Disrupting the
852 melanin-concentrating hormone receptor 1 in mice leads to cognitive deficits and alterations of NMDA
853 receptor function. The European journal of neuroscience. 2005;21(10):2837-44. Epub 2005/06/02.
854 82. Guo W, Allan AM, Zong R, Zhang L, Johnson EB, Schaller EG, et al. Ablation of Fmrp in adult
855 neural stem cells disrupts hippocampus-dependent learning. Nature Medicine. 2011;17(5):559-65.
856 83. Hersh JH, Saul RA. Health Supervision for Children With Fragile X Syndrome. Pediatrics.
857 2011;127(5):994-1006.
858 84. Lee B, Panda S, Lee HY. Primary Ciliary Deficits in the Dentate Gyrus of Fragile X Syndrome.
859 Stem Cell Reports. 2020;15(2):454-66.
860 85. Lee JW, Lee EJ, Hong SH, Chung WH, Lee HT, Lee TW, et al. Circling mouse: possible animal
861 model for deafness. Comparative medicine. 2001;51(6):550-4. Epub 2002/04/02.
862 86. Soken H, Robinson BK, Goodman SS, Abbas PJ, Hansen MR, Kopelovich JC. Mouse
863 cochleostomy: a minimally invasive dorsal approach for modeling cochlear implantation. The
864 Laryngoscope. 2013;123(12):E109-15. Epub 2013/05/16.
865 87. Yin TC, Britt JK, De Jesus-Cortes H, Lu Y, Genova RM, Khan MZ, et al. P7C3 neuroprotective
866 chemicals block axonal degeneration and preserve function after traumatic brain injury. Cell reports.
867 2014;8(6):1731-40. Epub 2014/09/16.
868 88. Ruxton GD. The unequal variance t-test is an underused alternative to Student's t-test and the
869 Mann–Whitney U test. Behavioral Ecology. 2006;17(4):688-90.
870 89. Delacre M, Lakens D, Leys C. Why Psychologists Should by Default Use Welch's t-test Instead
871 of Student's t-test. International Review of Social Psychology. 2017;30(1):92-101.
872 90. Zimmerman DW. A note on preliminary tests of equality of variances. The British journal of
873 mathematical and statistical psychology. 2004;57(Pt 1):173-81. Epub 2004/06/03.

874

875

876

877

878

Figures

879

880

881

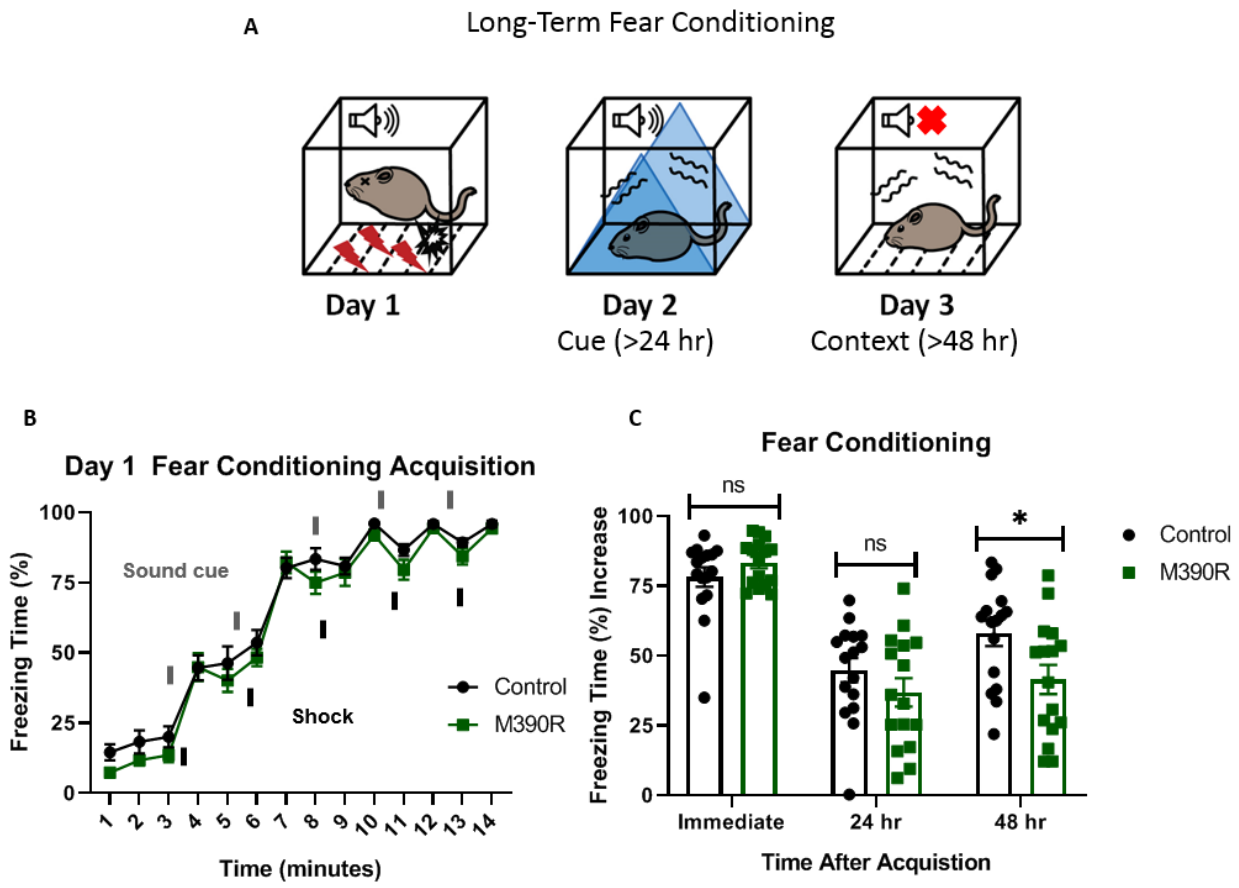

Fig 1. *Bbs1*$^{M390R/M390R}$ mice have impaired long-term context fear conditioning.

A.) Schematic diagram of the delay fear conditioning procedure. On the first day, a mouse was placed in a chamber, and a sound was paired with a shock multiple times. On the second day, a mouse was placed in an altered chamber. The chamber was triangle shaped (represented by the blue triangle) with a smooth floor, and a sound was given to test long-term cue fear conditioning. On the third day, the mouse was placed back in the same chamber (context) as day 1, without a sound cue. This set up was used to test long-term context fear conditioning.

B.) Day 1 acquisition between the control mice (n=16) and the *Bbs1*$^{M390R/M390R}$ mice (n=16) for long-term fear conditioning differed significantly (2-way ANOVA, time X genotype, $F(13, 420) = 0.4488$, $P=0.950$, time, $F(13, 420) = 179.8$, $P<0.0001$, genotype, $F(1, 420) = 11.46$, $P=0.0008$). The thick lines above the

893 curve indicate when the sound cue was given, and the thick lines below the curve indicate when the shock
894 was given.

895 C.) The immediate fear conditioning indicates training to the day 1 fear conditioning. The immediate fear
896 conditioning was measured as the difference of the freezing time (%) just before conditioning (first three
897 minutes) and just after conditioning (last minute). The immediate fear conditioning did not differ
898 significantly between the control mice (n=16) and *Bbs1*$^{M390/M390R}$ mice (n=16) used for long-term fear
899 conditioning (Welch's t-test, P=0.2107). The post 24 hr fear conditioning represents cue fear
900 conditioning, and is portrayed as Day 2 on the schematic diagram. The 24 hr fear conditioning (cue) was
901 measured as the difference of the freezing time (%) before the tone (cue) on day 2 and during the tone
902 (cue) on day 2. The 24 hr fear conditioning (cue) did not differ significantly between the control mice
903 (n=16) and the *Bbs1*$^{M390R/M390R}$ mice (n=16) (Welch's t-test, P=0.2414). The post 48 hr fear conditioning
904 represents context fear conditioning, and is portrayed as Day 3 on the schematic diagram. The 48 hr fear
905 conditioning was measured as the difference of the freezing time (%) just before conditioning (first three
906 minutes of day 1) and during the context on day 3. The 48 hr fear conditioning (context) between the
907 control mice (n=16) and the *Bbs1*$^{M390R/M390R}$ mice (n=16) differed significantly (Welch's t-test, P=0.0240).

908 control mice= *Bbs1*$^{M390R/+}$ mice, M390R=*Bbs1*$^{M390R/M390R}$ mice, hr = hour, ns = not significant * P< 0.05,
909 ** P< 0.01, ***P<0.001 ****P<0.0001

910

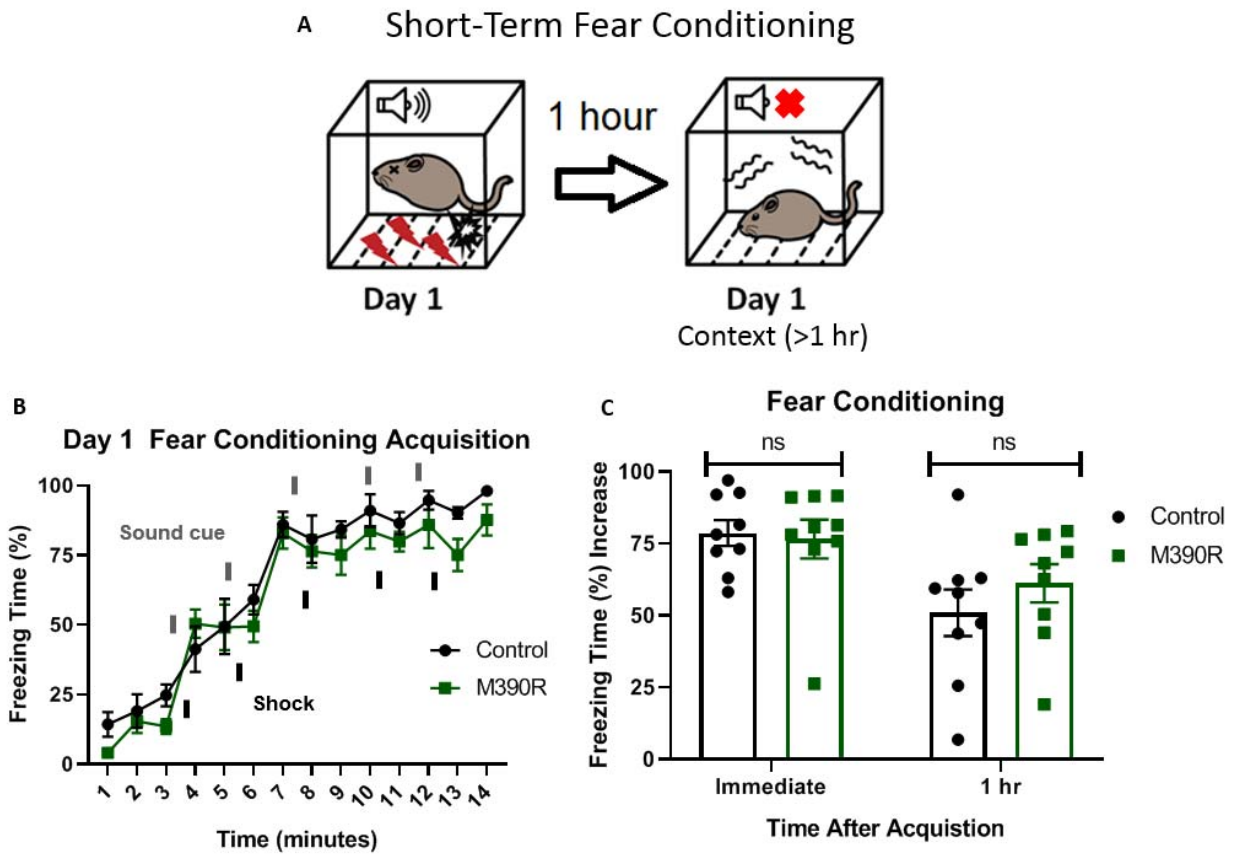

Fig 2. *Bbs1*$^{M390R/M390R}$ mice have normal short-term context fear conditioning.

A.) Schematic diagram of the one day delay fear conditioning procedure. On the first day, a mouse was placed in a chamber, and a sound was paired with a shock multiple time. One hour later, the mouse was placed back in the chamber, and freezing was measured for short-term context fear conditioning.

B.) Day 1 acquisition between the control mice (n=9) and the *Bbs1*$^{M390R/M390R}$ mice (n=9) used for the short term fear conditioning differed significantly (2-way ANOVA, time X genotype, F (13, 224) = 0.5574 , P=0.8858, time, F (13, 224) = 56.19, P<0.0001, genotype, F (1, 224) = 9.369, P=0.0025). The thick lines above the curve indicate when the sound cue was given, and the thick lines below the curve indicate when the shock was given.

C.) The immediate fear conditioning indicates training to the day 1 fear conditioning. The immediate fear conditioning was measured as the difference of the freezing time (%) just before conditioning (first three

minutes) and just after conditioning (last minute). The immediate fear conditioning did not differ significantly between control mice (n=9) and *Bbs1*$^{M390/M390R}$ mice (n=9) used for the short-term fear conditioning (Welch's t-test, P=0.8004). The 1 hr fear conditioning represents short-term context fear conditioning. The 1 hr fear conditioning was measured as the difference of the freezing time (%) just before conditioning and 1 hour after conditioning. The day 1 fear conditioning for context between the control mice (n=9) and the *Bbs1*$^{M390R/M390R}$ mice (n=9) did not reveal a significant difference (Welch's t-test, P=0.3436).

control mice= *Bbs1*$^{M390R/+}$ mice, M390R=*Bbs1*$^{M390R/M390R}$ mice, hr = hour, ns = not significant * P< 0.05, ** P< 0.01, ***P<0.001, ****P<0.0001

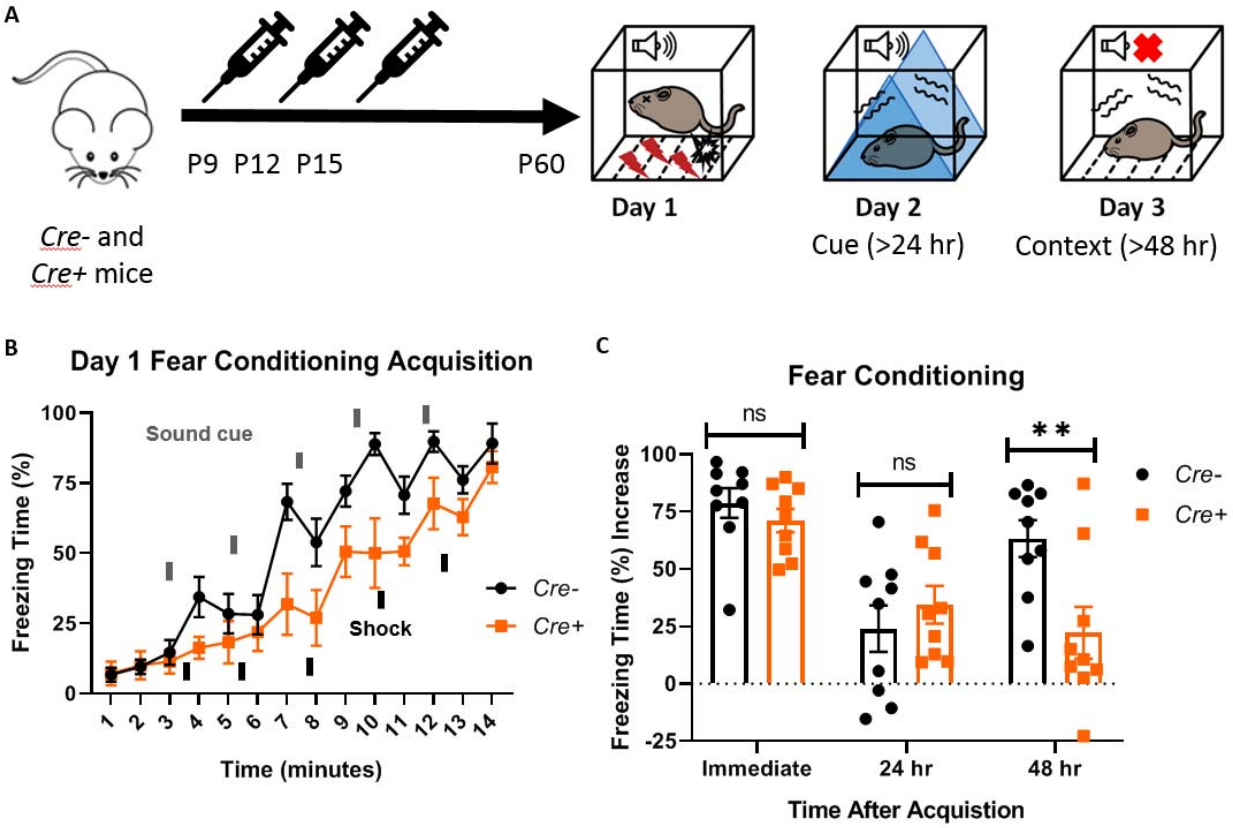

933

934 **Fig 3. Postnatal BBS genes are involved in long-term context fear conditioning.**

935 A.) Timeline of the tamoxifen I.P injections of the experimental mice, *Cre*+ (*Bbs8*$^{flox/-}$ and *Bbs8*$^{flox/flox}$;

936 *UBC-Cre*^{ERT2}) and littermate control mice, *Cre*- (*Bbs8*$^{flox/-}$ and *Bbs8*$^{flox/flox}$; *UBC-Cre*^{ERT2}-). To induce

937 *Bbs8* deletion in *Cre*+ mice, Tamoxifen was injected at P9, P12, and P15 (denoted by the syringe image).

938 At 2 months of age, the mice were tested for long-term fear conditioning. The first day was the

939 acquisition phase for fear conditioning, the second day was cue fear conditioning, and the third day was

940 context fear conditioning.

941 B.) Day 1 acquisition curve between the *Cre*- mice (n=9) and *Cre*+ mice (n=9) differed significantly (2-

942 way ANOVA, time X genotype, $F(13, 224) = 1.721$, $p=0.0579$, time, $F(13, 224) = 31.71$, $P<0.0001$,

943 genotype, $F(1, 224) = 39.16$, $P<0.0001$). The thick lines above the curve indicate when the sound cue

944 was given, and the thick lines below the curve indicate when the shock was given.

945 C.) The immediate fear conditioning indicates training to the day 1 fear conditioning. The immediate fear
946 conditioning was measured as the difference of the freezing time (%) just before conditioning (first three
947 minutes) and just after conditioning (last minute). The immediate fear conditioning did not differ
948 significantly between the *Cre*- mice (n=9) and *Cre*+ mice (n=9) used for long-term fear conditioning
949 (Welch's t-test, P=0.3717). The post 24 hr fear conditioning represents cue fear conditioning, and is
950 portrayed as Day 2 on the schematic diagram. The 24 hr fear conditioning (cue) was measured as the
951 difference of the freezing time (%) before the tone (cue) on day 2 and during the tone (cue) on day 2. The
952 24 hr fear conditioning (cue) did not differ significantly between the *Cre*- mice (n=9) and *Cre*+ mice
953 (n=9) (Welch's t-test, P=0.4325). The post 48 hr fear conditioning represents context fear conditioning,
954 and is portrayed as Day 3 on the schematic diagram. The 48 hr fear conditioning was measured as the
955 difference of the freezing time (%) just before conditioning (first three minutes of day 1) and during the
956 context on day 3. The 48 hr fear conditioning (context) between the *Cre*- mice (n=9) and *Cre*+ mice
957 (n=9) differed significantly (Welch's t-test, P=0.0099).

958 *Cre*- = *Bbs8*$^{flox/-}$ and *Bbs8*$^{flox/flox}$; *UBC-Cre*^{ERT2}- mice, *Cre*+ = *Bbs8*$^{flox/-}$ and *Bbs8*$^{flox/flox}$; *UBC-Cre*^{ERT2} +
959 mice, hr = hour, del=deletion, flx= flox, hr=hour, ns =not significant * P< 0.05, ** P< 0.01, ***P<0.001,
960 ****P<0.0001

961

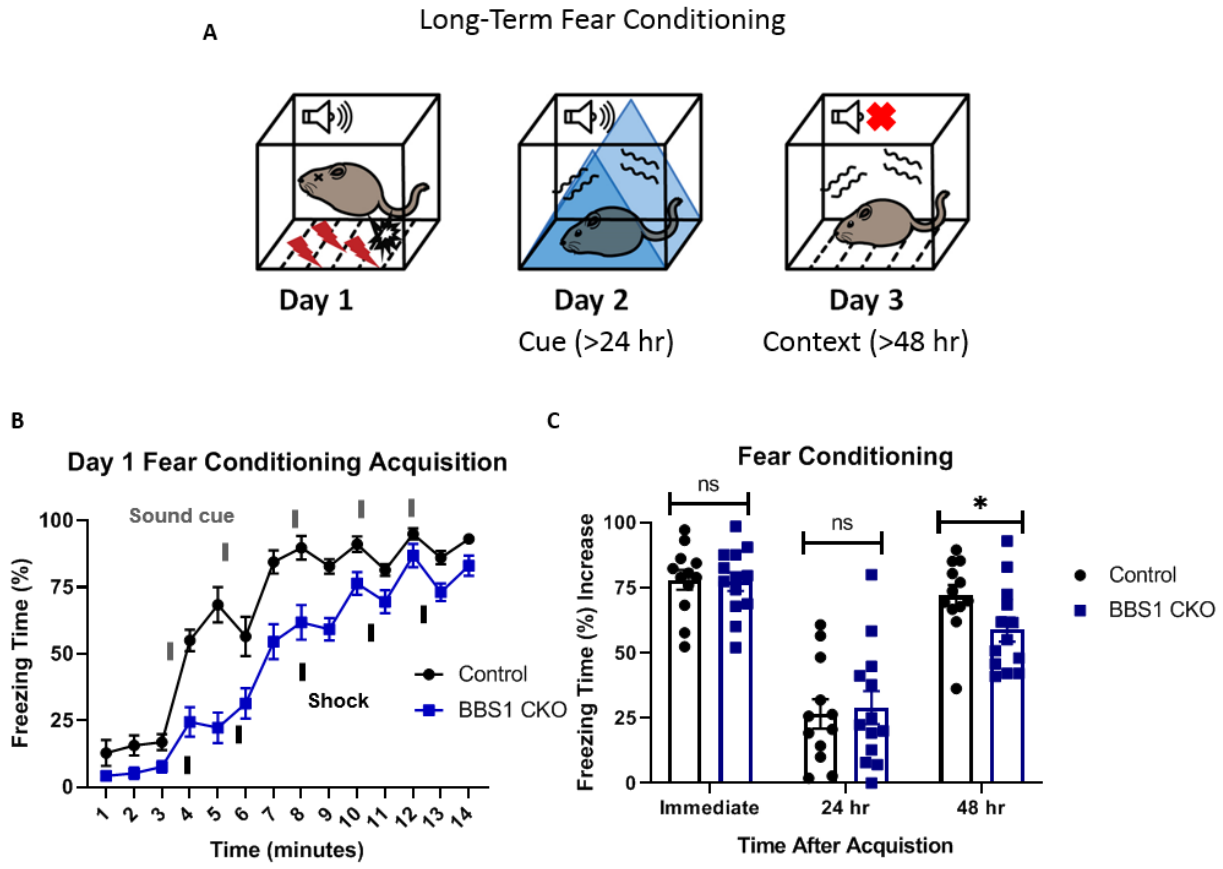

962

963 **Fig 4. BBS genes in the forebrain are involved in long-term context fear conditioning.**

964 A.) Schematic diagram of the three day delay fear conditioning procedure. On the first day, a mouse was

965 placed in a chamber, and a sound was paired with a shock multiple time. On the second day, a mouse was

966 placed in an altered chamber that was triangle shaped (represented by the blue triangle) with a smooth

967 floor, and a sound was given to measure cue fear conditioning. On the third day, the mouse was placed

968 back in the same chamber, and measured for freezing without sound. This gives the context fear

969 conditioning.

970 B.) Day 1 acquisition between the *Emx1-Cre* mice (control, mixed strain of C57BL/6 and 129/SVeV,

971 n=12) and the *Bbs1*$^{flox/-}$; *Emx1-Cre* (BBS1 CKO, mixed strain of C57BL/6 and 129/SVeV, n=13) differed

972 significantly (2-way ANOVA, time X genotype, $F(13, 322) = 3.483$, $P<0.0001$, time, $F(13, 322) =$

93.95, P<0.0001, genotype, F (1, 322) = 137.5, P<0.0001). The thick lines above the curve indicate when the sound cue was given, and the thick lines below the curve indicate when the shock was given.

C.) The immediate fear conditioning indicates training to the day 1 fear conditioning. The immediate fear conditioning was measured as the difference of the freezing time (%) just before conditioning (first three minutes) and just after conditioning (last minute). The immediate fear conditioning did not differ significantly between the control *Emx1-Cre* mice (n=12) and *Bbs1*$^{flox/-}$; *Emx1-Cre* (n=13) used for the long-term fear conditioning (Welch's t-test, P=0.8999). The post 24 hr fear conditioning represents cue fear conditioning, and is portrayed as Day 2 on the schematic diagram. The 24 hr fear conditioning (cue) was measured as the difference of the freezing time (%) before the tone (cue) on day 2 and during the tone (cue) on day 2. The 24 hr fear conditioning (cue) did not differ significantly between the control *Emx1-Cre* mice (n=12) and *Bbs1*$^{flox/-}$; *Emx1-Cre* (n=13) (Welch's t-test, P=0.7005). The post 48 hr fear conditioning represents context fear conditioning, and is portrayed as Day 3 on the schematic diagram. The 48 hr fear conditioning was measured as the difference of the freezing time (%) just before conditioning (first three minutes of day 1) and during the context on day 3. Day 3 fear conditioning for context between the control *Emx1-Cre* mice (n=12) and *Bbs1*$^{flox/-}$; *Emx1-Cre* (n=13) differed significantly (Welch's t-test, P=0.0438, Mann-Whitney-Wilcoxon Test, P=0.0398).

control = *Bbs1*$^{+/+}$; *Emx1*-Cre mice, BBS1 CKO = *Bbs1*$^{flox/-}$; *Emx1-Cre*+ mice, hr=hour, ns =not significant * P< 0.05, ** P< 0.01, ***P<0.001, ****P<0.0001

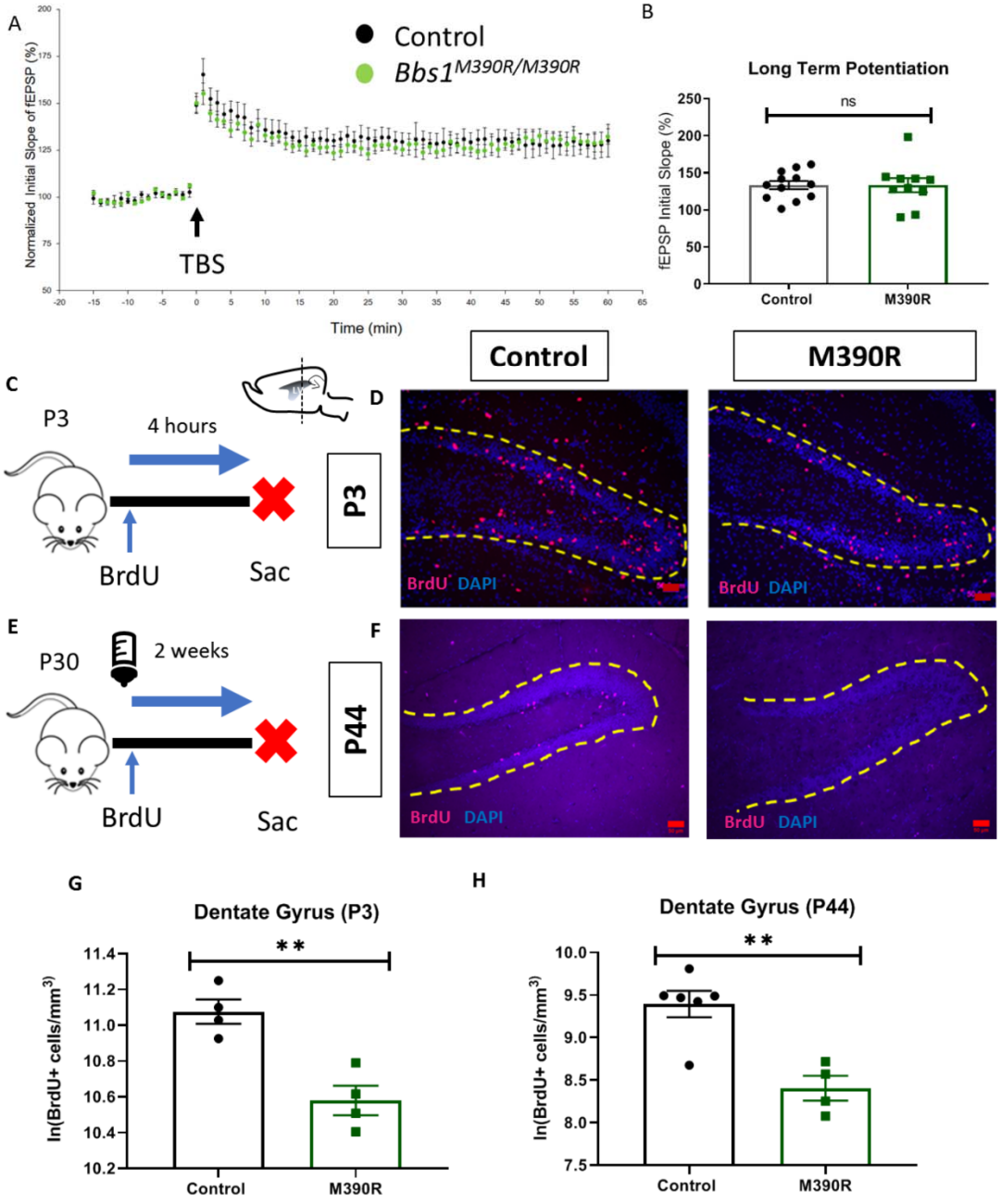

993

994 **Fig 5. *Bbs1*$^{M390R/M390R}$ mice have decreased hippocampal proliferation.**

A.) Normalized initial slope (%) recordings of field excitatory post synaptic potentials (fEPSP) in the hippocampal CA1 Schaffer-collateral pathway between 2 month male control mice (n=17, 4 mice) and *Bbs1*$^{M390R/M390R}$ mice (n=16, 4 mice). LTP was induced by 12 theta burst stimulation (TBS).

B.) The Long Term Potentiation (average of last five minutes of normalized initial slope of fEPSP) in the hippocampal CA1 Schaffer-collateral pathway between 2 month male control mice (n=17, 4 mice) and *Bbs1*$^{M390R/M390R}$ mice (n=16, 4 mice) did not differ significantly (Welch's t-test, P=0.8407).

C.) Schematic diagram of the BrdU injections of postnatal day 3 (P3) mice. P3 mice were IP injected with 300mg/kg BrdU, and taken down four hours later. Sac=Sacrifice

D.) Inverted fluorescent microscope images of the P3 Dentate Gyrus. The sections were stained with Bromodeoxyruidine (BrdU) and counterstained with the nuclear marker, DAPI. The yellow dotted line outlines the dentate gyrus. The Red Bar line was 50um.

E.) Schematic diagram of the BrdU procedures for postnatal day 44 (P44) mice. At P30, mice were started on BrdU injections (2x50mg/kg) for five days. At P44, mice were taken down. Sac=Sacrifice

F.) Inverted fluorescent microscope images of the P44 Dentate Gyrus. The sections were stained with Bromodeoxyruidine (BrdU) and counterstained with the nuclear marker, DAPI. The yellow dotted line outlines the dentate gyrus. The Red Bar line was 50um.

G.) Decreased proliferation in the dentate gyrus of P3 *Bbs1*$^{M390R/M390R}$ mice. The natural logarithm of BrdU+cell/mm^3 in the dentate gyrus between the control mice (n=4) and the *Bbs1*$^{M390R/M390R}$ mice (n=4) differed significantly (Welch's t-test, P=0.0038).

H.) Decreased proliferation in the dentate gyrus of P44 *Bbs1*$^{M390R/M390R}$ mice. The natural logarithm of BrdU+cell/mm^3 in the dentate gyrus between the control mice (n=6) and the *Bbs1*$^{M390R/M390R}$ mice (n=4) differed significantly (Welch's t-test, P=0.0018).

control=*Bbs1*$^{+/+}$, *Bbs1*$^{M390R/+}$ mice, M390R=*Bbs1*$^{M390R/M390R}$ mice, hr=hour, ns=not significant, * P< 0.05, ** P< 0.01, ***P<0.001, ****P<0.0001

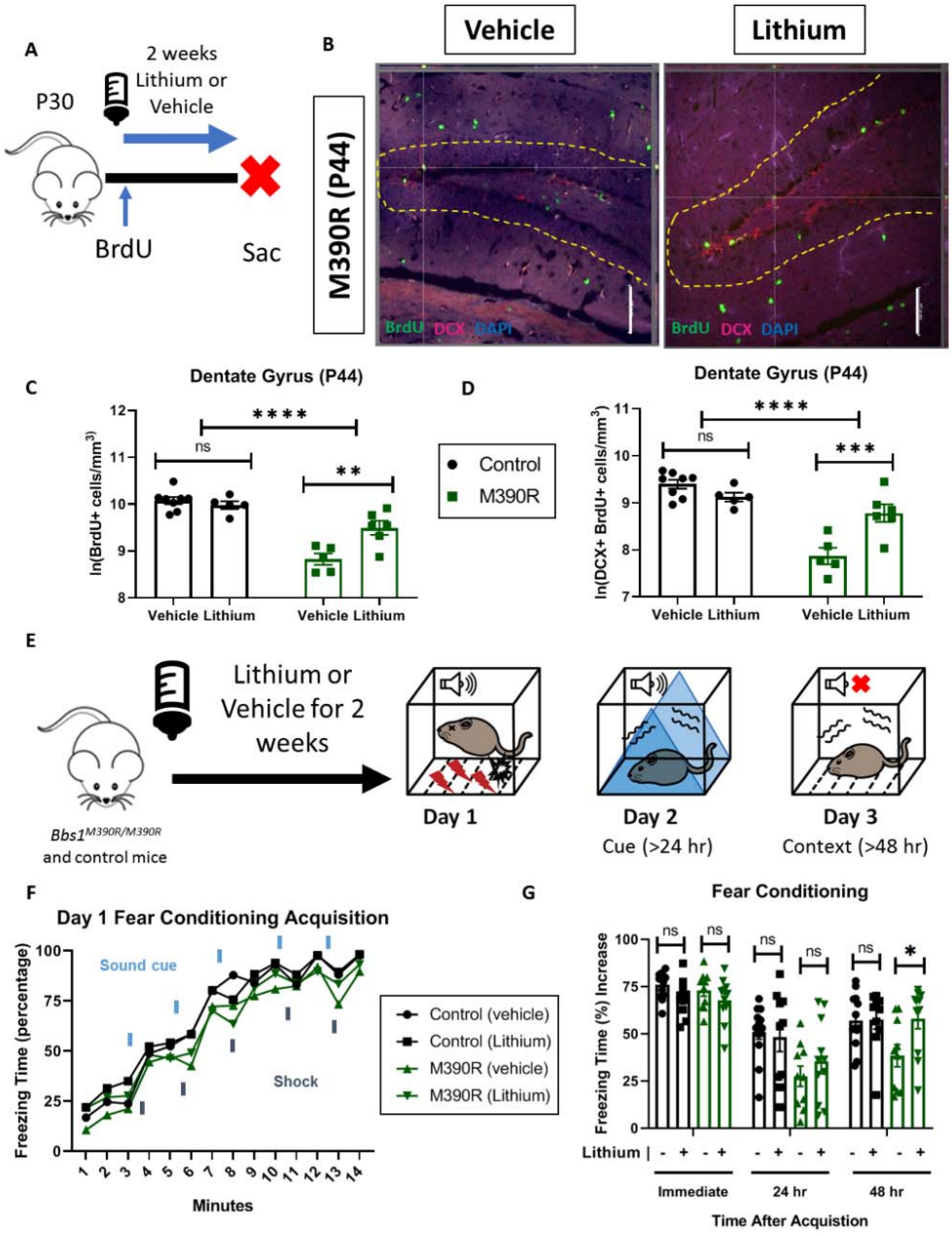

1019

1020 **Fig 6. Chronic Lithium treatment rescued long-term context fear conditioning in *Bbs1*$^{M390R/M390R}$**

1021 **mice.**

A.) Schematic diagram of the Bromodeoxyuridine (BrdU) procedures for postnatal day 44 (P44) mice. At P30, mice were started on Lithium water (45mM) or continued with water (vehicle). Mice were also started on BrdU injections (2x50mg/kg) for five days. At P44, mice were taken down. Sac=Sacrifice

B.) Images of immunohistochemistry for neurogenesis of vehicle and lithium treated *Bbs1*$^{M390R/M390R}$ mice. Z-stack, 20X, images of Dentate Gyrus at postnatal day 44 (P44). The tissue sections were stained with BrdU, Doublecortin (DCX), and counterstained with the nuclear marker DAPI. The yellow dotted line outlines the dentate gyrus. The White Bar line indicates 100micrometers.

C.) Proliferation in the dentate gyrus of P44 control and *Bbs1*$^{M390R/M390R}$ mice. We assessed two factors, and found a significant interaction for genotype and treatment, and a difference in treatment and genotype (2-way ANOVA, treatment X genotype, $F(1, 20) = 6.428$, $P=0.0026$, treatment, $F(1, 20) = 1.569$, $P=0.0177$, genotype, $F(1, 20) = 46.89$, $P<0.0001$). A Sidak's multiple comparisons test showed a significant difference in treatment for *Bbs1*$^{M390R/M390R}$ mice (n=5 Vehicle, n=6 Lithium, $P=0.7875$) but not for control mice (n=8 Vehicle, n=5 Lithium, $P=0.0010$)

D.) Neurogenesis in the dentate gyrus of P44 control and *Bbs1*$^{M390R/M390R}$ mice. We assessed two factors, and found a significant interaction between genotype and treatment, and a difference in treatment and genotype (2-way ANOVA, treatment X genotype, $F(1, 20) = 11.37$, $P=0.0005$, treatment, $F(1, 20) = 0.0368$, $P=0.5779$, genotype, $F(1, 20) = 29.54$, $P<0.0001$). A Sidak's multiple comparisons test showed a significant difference in treatment for *Bbs1*$^{M390R/M390R}$ mice (n=5 Vehicle, n=6 Lithium, $P=0.0006$) but not for control mice (n=8 Vehicle, n=5 Lithium, $P=0.3301$).

E.) Timeline of LiCl treatment. At 4-5 weeks of age, mice were treated with LiCl (45mmol) water or continued on water (vehicle). After two weeks of treatment, mice were tested on a 3 day fear conditioning set up. Day 1 was the training (acquisition phase) for fear conditioning. The second day was testing for cue fear conditioning. The third day was testing for context fear conditioning.

F.) Day 1 fear conditioning acquisition between the vehicle treated control mice (n=13) and *Bbs1*$^{M390R/M390R}$ (45mmol) treated mice (n=10), and lithium treated control mice (n=9) and *Bbs1*$^{M390R/M390R}$ (45mmol) treated mice (n=11). Graph was presented without standard error. We found a significant

difference in Treatment, Genotype, and Time (3-way ANOVA, Time x Genotype x Treatment, F (13, 560) = 0.2572, P=0.9963; Genotype x Treatment, F (1, 560) = 0.4214, P=0.5165; Time x Treatment, F (13, 560) = 1.338, P=0.1860; Time x Genotype, F (13, 560) = 0.5960, P=0.8582; Treatment, F (1, 560) = 5.475, P=0.0196; Genotype, F (1, 560) = 39.48, P<0.0001; Time, F (13, 560) = 157.3, P<0.0001). The thick lines above the curve indicate when the sound cue was given, and the thick lines below the curve indicate when the shock was given.

G.) The immediate fear conditioning indicates training to the day 1 fear conditioning. The immediate fear conditioning was measured as the freezing time (%) increase of the freezing time (%) just after conditioning (last minute) to the freezing time (%) just before conditioning (first three minutes). The immediate fear conditioning was not significantly different between the control mice given vehicle (n=13) and control mice given LiCl water (n=10) (Welch's t-test, P=0.0689) and did not significantly differ between the *Bbs1*$^{M390R/M390R}$ mice given vehicle (n=10) and *Bbs1*$^{M390R/M390R}$ mice given LiCl water (45mmol) (n=11) (Welch's t-test, P=0.2834).

The post 24 hr fear conditioning represents the cue fear conditioning. The 24 hr fear conditioning (cue) was measured as the freezing time (%) increase of the freezing time (%) during the tone (cue, day 2) to the freezing time (%) before the tone (cue, day 2). The 24 hr fear conditioning (cue) was not significantly different between the control mice given vehicle (n=13) and control mice given LiCl water (n=10) (Welch's t-test, P=0.7483) and was not significantly different between the *Bbs1*$^{M390R/M390R}$ mice given vehicle (n=10) and *Bbs1*$^{M390R/M390R}$ mice given LiCl water (45mmol) (n=11) (Welch's t-test, P=0.3625).

The post 48 hr fear conditioning represents the context fear conditioning. The 48 hr fear conditioning was measured as the freezing time (%) increase of the freezing time (%) during the context on day 3 to the freezing time (%) just before conditioning (first three minutes of day 1). Day 3 fear conditioning for context was not significantly different between the control mice given vehicle (n=13) and control mice given LiCl water (n=10) (Welch's t-test with Bonferroni correction, P=0.9285) but was significantly different between the *Bbs1*$^{M390R/M390R}$ mice given vehicle (n=10) and *Bbs1*$^{M390R/M390R}$ mice given LiCl water (45mmol) (n=11) (Welch's t-test, P=0.0235).

1074 control=*Bbs1*$^{+/+}$, *Bbs1*$^{M390R/+}$ mice, M390R=*Bbs1*$^{M390R/M390R}$ mice, hr=hour, ns=not significant, * P< 0.05,

1075 ** P< 0.01, ***P<0.001, ****P<0.0001

1076